Yale Postdoctoral Association

The YPA Presents

the

2025 Yale Postdoctoral Association Symposium

at OC Marsh Lecture Hall

Yale University

New Haven, CT

June 6, 2025

Contents

The Yale Postdoctoral Association would like to thank the following sponsors for their generous support

STEMCELL™ TECHNOLOGIES

ThermoFisher SCIENTIFIC

fisher scientific

Stop by their tables in the lobby to learn more about industry opportunities!

*We also thank the **Yale Office for Postdoctoral Affairs** for their annual support of our programming*

Schedule

Registration/Poster set up - 8:10-8:30 am

Opening Remarks - 8:30-8:45 am

Chair: Jacob Orkwis and Adati Tarfa

1st Session - 8:45 am- 9:15 am

Format: (5) 5-minute lightning talks (4 min talk + 1 min Q&A)

Chair: Gizem Nur Sahin Kayabolen

TIME	Presenter	Title
8:45 – 8:50	**Aliaksandr Kishchanka**	***Analyzing Yale University Reproductive Sciences Biobank Data vs. the General Population: Identifying Gaps and Advancing Equitable Representation***
8:50 – 8:55	**Sheila Nagamatsu**	***Association of PTSD Symptom Trajectories with Accelerated Pace of Epigenetic Aging in U.S. Military Veterans***
8:55 – 9:00	**Jennifer Park**	***Brain-based prediction of gaming disorder in adolescents***
9:00-9:05	**Luis Mestre**	***Increasing Trends of Polysubstance Use among Lesbian and Bisexual US Female Adults***

9:05 – 9:10	**Caroline Muiler Barbosa Nogueira**	***Role of CFTR in SGK1 and stress-induced signaling in mouse intestine***

2nd Session - 9:15 am-9:45 am

Format: (3) 10-minute short talks (8 min talk + 2 min Q&A)

Chair: Jon Bell

TIME	Presenter	Title
9:15-9:25	**Shubham Misra**	***Cross-platform proteomics and machine learning algorithms nominate biomarkers of stroke diagnosis***
9:25-9:35	**Dilpreet Kour**	***A Comparative Analysis of Protein Interactors of Kv1.3 in Microglia and T-Cells: Implications for Neurodegenerative and Autoimmune Diseases***
9:35-9:45	**Bruno Batinica**	***Artificial Intelligence Enhanced Cardiovascular Disease Prediction Using Electrocardiogram Images***

Coffee break - 9:45-10:15 am

3rd Session - 10:15 am- 11:20 am

Format: (6) 10-minute short talks (8 min talk + 2 min Q&A)

Chair: Chetna Dhembla

Time	Presenter	Title
10:15 – 10:25	**Kelli Connolly**	***Impact of LKB1 co-mutation in lung cancer on the functionality of antitumor T cells***
10:25 – 10:35	**Cem Demirkiran**	***Preclinical efficacy of the estrogen receptor degrader fulvestrant in combination with RAF/MEK clamp avutometinib and FAK inhibitor in low-grade serous ovarian cancer with acquired resistance to chemotherapy and aromatase Inhibitor***
10:35 – 10:45	**Eman Salih**	***Access to Chronic Non-Communicable Disease Medications During Wartime in Sudan***
10:45 – 10:55	**José Martínez-Magaña**	***Dissecting the ancestry-specific genetic architecture of alcohol consumption in Latin American Individuals***
10:55 – 11:05	**Afsheen Nasir**	***Sex-Based Disparities in Thoracic Aortic Disease***
11:05 – 11:15	**Nebal Abu Hussein**	***Molecular Networks in Silicosis: Transcriptomics Analysis in Exposure driven Pulmonary Fibrosis***

4th Session - 11:20 am-12:00 pm

Format: (6) 5-minute lightning talks (4 min talk + 1 min Q&A)

Chair: Nebal Abu Hussein

TIME	Presenter	Title
11:20-11:25	**Rizwana Afroz**	***Endothelial-specific LRP5 deletion mitigates atherosclerosis***
11:25-11:30	**Michele D'Agata**	***Adoptive Transfer of Preeclampsia-Exposed T Cells Increases Blood Pressure and Arterial Stiffness Without Microvascular Alterations Following Repeated Hypertensive Stimuli in Female Mice***
11:30-11:35	**Johnathan Hoggarth**	***A Simple Method for Generating Droplets on a Vibrating Liquid Bath***
11:35-11:40	**Pratap Vydyam**	***Tick-Tock: Tafenoquine vs. Malaria and Babesiosis***
11:40-11:45	**Chetna Dhembla**	***Insights into the nuclear import of 26S proteasomes using a nuclear pore complex (NPC) mimic system***
11:45-11:50	**Sumon Sarkar**	***Collective intelligence of specialized language models guides de novo chemical synthesis***

Lunch and Poster Session - 12:00-2:00 pm.

5th Session - 2:00 pm- 3:00 pm

Format: (6) 10-minute short talks (8 min talk + 2 min Q&A)

Chair: Cameron Gardner

TIME	Presenter	Title
2:00-2:10	**Tiantian Gong**	***Disincentivize Collusion in Verifiable Secret Sharing***
2:10-2:20	**Henrique Oliva**	***Sleep Alterations in Opioid Use Disorder: A Systematic Review and Meta-Analysis***
2:20-2:30	**Ling Xu**	***Molecular insights into de novo small molecule recognition by an intron RNA structure***
2:30-2:40	**Peng Xu**	***NAT10 drives brain metastasis by regulating the serine synthesis pathway***
2:40-2:50	**Mark Williams**	***Larp1 supports brain growth and spatial memory through post-transcriptional control of the translation machinery***
2:50-3:00	**Yaru Xu**	***Genome-wide CRISPRi Screen Identifies lncRNA CRNDE as a regulator of Lineage Plasticity in Prostate Cancer***

Title IX Fireside Chat/Coffee Break - 3:00 pm- 3:30 pm

Panel Session - 3:30 pm-5:00 pm

The Pivot: Stories of transition from academia to industry

- ***Karen Perez de Arce, PhD, Principal Scientist II, Novartis***
- ***Aarti Sharma, PhD, Director-Motor Neuron Diseases, Regeneron***
- ***Christopher Barbieri, PhD, Associate Director, Bristol Myers Squibb***

Moderator: Montrell Seay, PhD, Senior Associate Director of STEM Employer Relations, Office of Career Strategy (OCS)

Submit your questions here!

Keynote Talk - 5:00 pm- 6:00 pm

"Don't Panic and always carry a towel - lessons from my accidental career"

Naftali Kaminski, MD (Section Chief, Pulmonary, Critical Care & Sleep Medicine, Yale School of Medicine)

Session Host: Jacob Orkwis, Adati Tarfa

Cultural Performance - 6:00 pm-6:30 pm

Session Host: Dilpreet Kour

- *"Pearls & Jade Within: A Vocal Odyssey of Science, Art & Self Discovery*- by **Haoyang Wei**
- *"Mysterious waves: the sound that changes you"* **by Sajad Nezhadian**
- *"An unplugged Sufi-Rock Rendition"*- **by Shubham Misra**
- *"Swungover with Yale swing, Blues & Fusion (YBSF)"* **by YBSF**
- *"Fragments of a Familiar Tune"* by **Namrata Sethi**
- *"Tangled in Tango"*-**Tiffany Chang & Michelle Wong**

Reception: Awards and Closing Remarks - 6:30 pm- 7:15 pm

Afterparty: Gryphon's Pub, 7:30 pm - Late

Finding Marsh Lecture Hall

OC Marsh Lecture Hall at Yale Science Building can be found at Yale University, ***260 Whitney Ave, New Haven, CT 06511***

Please see the following visual guides for navigating Science Hill during the current construction. The first map also highlights available, meter-by-hour street parking nearby. Free parking may also be found on Humphrey St., Bishop St., and Edwards St. further from Science Hill.

Entrance to Marsh Hall | Street parking options | Peabody Parking | Directions to Marsh Hall Entrances | Directions to Bass Loading Dock

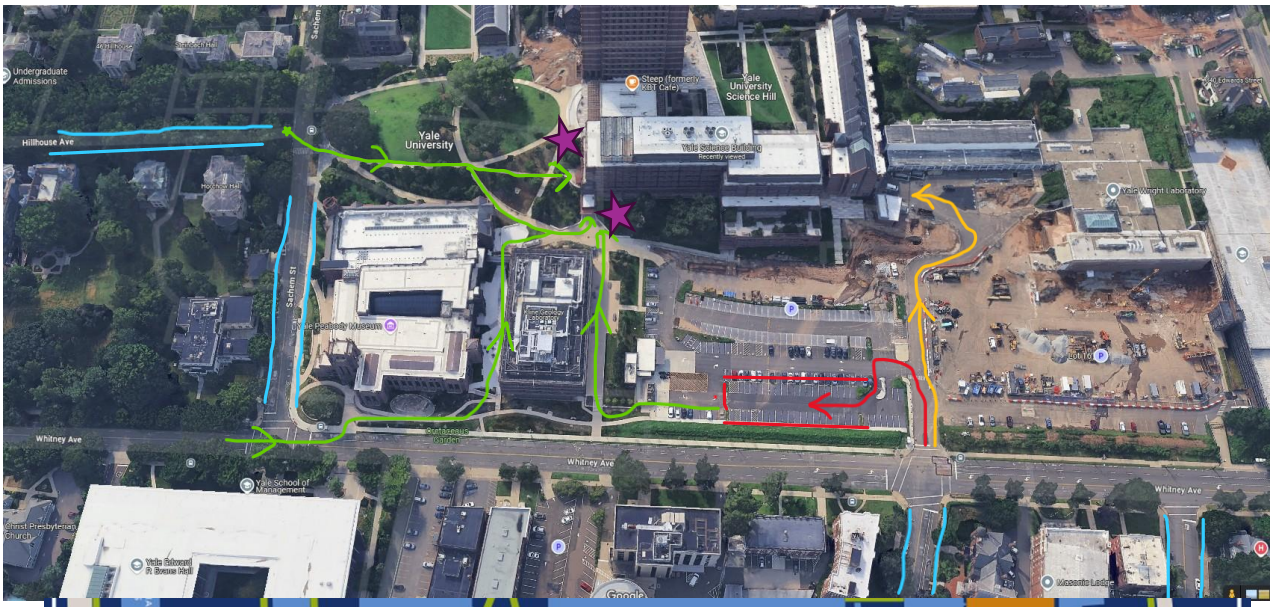

Alternative Parking

There is also street parking available that requires small payments using coin-operated meters or the Park Mobile app. Hillhouse Ave has nice availability and is a short walk to Marsh. Free parking may also be found on Humphrey St., Bishop St., and Edwards St., but will likely place you further away from Science Hill.

Building Entrance

- Marsh Hall can be **accessed on the first level**: (41.316884, -72.921652)
- Or on the **second floor**: (41.316869, -72.921928)
- Additional entrances are found on the other side of YSB, but require navigation through the building to access Marsh.

Programming

[Submit your panel questions here](#)!


Yale Postdoctoral Association
Join us at the
5 - 6 PM June 6th at O.C. Marsh Hall
8th Annual YPA Symposium
Presenting
Naftali Kaminski, MD
Key Note Speaker
Register
FOR THE SYMPOSIUM
Don't panic and always carry a towel:
Lessons of my Accidental Career

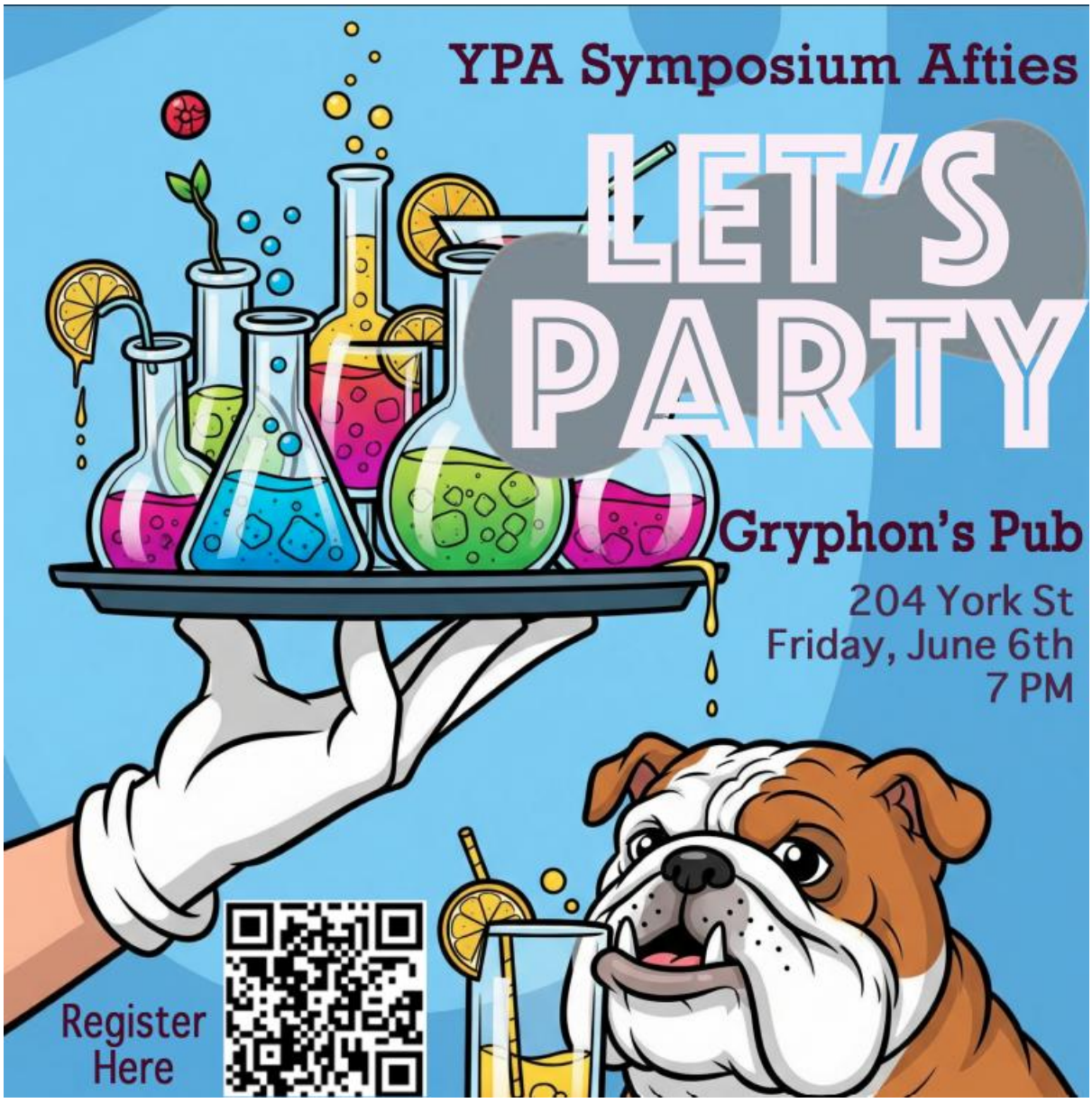
YPA Symposium Afties
LET'S PARTY
Gryphon's Pub
204 York St
Friday, June 6th
7 PM
Register Here


Yale Postdoctoral Association
Help us design the official poster for next year's symposium! We are looking for original artwork that captures the spirit of science, discovery, and the postdoc experience at Yale.
2026 Postdoc Symposium
ART Contest
Register Here
Submission Guidelines
Theme: Yale University, science/discovery, postdoc community
Who Can Enter: All Yale-affiliated postdocs
Submission Formats: Digital designs, scanned hand-drawings, original photography
Deadline: Submit your artwork by Sept 30th 2025
Prize: Featured as the official 2026 YPA Symposium poster, recognition across Yale Channels, and a SPECIAL PRIZE
Dr. Dan
YALE

Selected 10-Minute Talks

Sleep Alterations in Opioid Use Disorder: A Systematic Review and Meta-Analysis

Henrique Olivia

With Tiago Paiva Prudente, MD; Alisson M. Paredes Naveda, BS; Renato Sobral Monteiro-Junior, PhD; Marc N. Potenza, MD, PhD; Peter T. Morgan, MD, PhD; Gustavo A. Angarita, MD, MHS

Background: Opioid use disorder (OUD) has been consistently linked to disturbances in sleep, which may worsen the physical and mental health outcomes associated with chronic opioid use. These sleep disruptions can contribute to increased cravings, relapse risk, and hindered recovery. Despite their clinical importance, the specific effects of OUD on objective sleep parameters warrants further investigation. This meta-analysis aims to quantify the impact of OUD on polysomnography-derived sleep metrics. Methods: We conducted a systematic review and meta-analysis of studies examining objective sleep outcomes in individuals with OUD, PROSPERO (CRD42024531160). Searches were performed across Embase, PsycINFO, PubMed, Scopus, and Web of Science up to April 2025. Studies included adult participants with a history of chronic opioid use, compared to opioid-naïve controls. Only studies using objective measures of sleep (i.e., polysomnography) were included. Sleep data were synthesized using mean differences (MD) and 95% confidence intervals (CI). Results: Of 971 studies screened, three met inclusion criteria (one from India, and two from Egypt). These studies included 68 male participants with OUD and 45 male controls, with participant ages ranging from 18 to 45 years. Sleep assessments occurred at least one week after last opioid use in two studies. OUD was significantly associated with reduced total sleep time (TST) (MD: -38.16 minutes, 95% CI: -63.04 to -13.28). No significant differences were observed in percentage of Rapid Eye Movement (REM) sleep (MD: 0.19, 95% CI: -0.15 to 0.53), REM latency (MD: 6.52, 95% CI: -21.19 to 34.23), slow-wave sleep (SWS) (MD: 0.81, 95% CI: -6.01 to 7.64), or sleep efficiency (MD: -24.83, 95% CI: -54.43 to 2.76). Wake after sleep onset could not be analyzed due to insufficient data. The overall risk of bias across studies was rated as moderate. Conclusions: OUD is associated with significantly reduced TST. Although there were trends toward decreased sleep efficiency, these did not reach statistical significance. No consistent associations were found for REM sleep or SWS. Given the limited data, this is clearly an area where more studies are needed, particularly studies that use tools not only capable of detecting TST alterations but also feasible for use in clinical settings (e.g., actigraphy). Emerging evidence suggests that agents such as orexin antagonists, which may help prolong TST, could offer promising treatment avenues. Future studies should also explore the relationship between sleep disturbances and relapse in order to guide more targeted interventions.

Cross-platform proteomics and machine learning algorithms nominate biomarkers of stroke diagnosis

Shubham Misra

With Aditya Natu, Prateek Kumar, Rolando Garcia-Milian, Caroline M. Watson, Michael R. Frankel, Srikant Rangaraju

Background: Blood-based biomarkers of stroke diagnostic groups, namely acute ischemic stroke (AIS), intracerebral hemorrhage (ICH), transient ischemic attack (TIA) or stroke mimics (MIM), can be valuable in emergency settings for triage and treatment decisions. We aimed to nominate plasma protein biomarkers of stroke diagnostic groups in acute settings using cross-platform proteomics. Methods: We

conducted a single center case-control study using a prospective plasma repository from 2010 to 2014. We included patients aged ≥18 years with a suspected stroke diagnosis and collected plasma in the emergency room before administering any therapeutic intervention. Our primary outcome was differentially enriched proteins (DEPs) comparing AIS, ICH, TIA, and MIM. We performed aptamer-based discovery proteomics using the plasma 7K SomaScan assay. Top DEPs were nominated in pairwise analyses using a combination of fold-change and significance, Boruta random forest feature selection, and variance partitioning analyses, adjusting for clinical covariates. Multigroup analyses were performed using sparse partial least squares discriminant analysis (sPLS-DA). Internal validation was performed using targeted mass spectrometry proteomics (BAK-270). Results: We included 100 patients (mean age 58.5 years, 44% males) comprising 40 AIS, 20 ICH, 20 TIA, and 20 MIM. SomaScan quantified 7307 protein targets of which 58 nominated proteins differentiated the stroke subtypes, majority of which (21/58) differentiated MIM from AIS, ICH, and TIA. We identified a panel of 7 proteins as top classifiers for AIS (area under the curve (AUC): 0.82, negative predictive value (NPV): 75%), 5 for ICH (AUC 0.88, NPV: 94.5%), 6 for TIA (AUC 0.94, NPV: 98.5%), and 8 for MIM (AUC 0.94, NPV: 94.4%). In the validation phase, targeted proteomics validated 11 proteins including VTN and PLG as top MIM classifiers. Conclusions: This study highlights plasma proteomics as a valuable tool for discovering protein biomarkers of stroke diagnosis. External validation is warranted to validate these findings in larger, multi-center cohorts.

Larp1 supports brain growth and spatial memory through post-transcriptional control of the translation machinery.

Mark Williams

With Maegan J. Watson, and Carson C. Thoreen

In the brain, tight regulation of the translation of mRNAs is essential for development and plasticity. The production of the translation machinery itself can be controlled by the mTOR signaling pathway, a regulator of growth, through the post-transcriptional regulation of mRNAs with terminal oligopyrimidine (TOP) motifs. These mRNAs encode nearly all ribosomal proteins and other key translation factors. While TOP mRNAs are broadly expressed, they are particularly enriched in distal compartments such as axons, dendrites and synapses, suggesting local functions for their regulation. To understand how TOP mRNA regulation impacts the brain, we generated mice with a brain-specific deletion of Larp1, the mTOR effector that directly regulates TOP mRNAs. The loss of Larp1 significantly decreases brain mass and reduces the density of neurons. Global levels of TOP mRNAs are depleted by more than 50%. This depletion is even greater at synapses, reversing the enrichment that is normally observed. In behavior tests, Larp1-deficient mice are severely impaired in spatial learning and memory. These observations demonstrate a critical role for Larp1 in regulation of the global and local synthesis of the translation machinery, and that disruption impairs neuronal growth and functions involved in learning and memory.

Genome-wide CRISPRi Screen Identifies lncRNA CRNDE as a regulator of Lineage Plasticity in Prostate Cancer

Yaru Xu

Resistance to androgen receptor (AR)-targeted therapies remains a major clinical challenge in the management of metastatic castration-resistant prostate cancer (mCRPC). Emerging evidence highlights

lineage plasticity—the ability of tumor cells to transition from an AR-dependent luminal state to alternative, AR-independent phenotypes—as a key driver of therapy resistance. However, the non-coding regulatory mechanisms that enable this phenotypic shift remain poorly defined. Through an unbiased genome-wide CRISPR interference (CRISPRi) screen targeting ~10,000 long non-coding RNAs (lncRNAs), we identified Colorectal Neoplasia Differentially Expressed (CRNDE) as a top candidate whose loss confers resistance to AR-targeted therapies both in vitro and in vivo. Mechanistic studies revealed that CRNDE depletion induces therapy resistance by upregulating Procollagen-Lysine,2-Oxoglutarate 5-Dioxygenase 2 (PLOD2), a collagen-modifying enzyme that elevates intracellular succinate levels and activates neuroendocrine-like transcriptional program. Notably, genetic depletion of PLOD2 or pharmacologic suppression of succinate restores sensitivity to AR-targeted therapy and suppresses lineage plasticity in CRNDE-deficient models. These findings define a previously unrecognized lncRNA–metabolism–lineage axis that drives therapeutic resistance in prostate cancer and nominate CRNDE as a critical suppressor of lineage plasticity with translational relevance for overcoming resistance in advanced disease.

Acknowledgment: I would like to thank my principal investigator, Dr. Ping Mu, for his mentorship and guidance. I also thank the members of the Jiyeon Kim lab for their valuable input and support. This work was supported by NCI, PCF, CDMRP and CPRIT. Finally, I appreciate the organizers of the YPA for the opportunity to present my work.

Disincentivize Collusion in Verifiable Secret Sharing

Tiantian Gong

With Aniket Kate, Hemanta K. Maji, Hai H. Nguyen

In verifiable secret sharing (VSS), a dealer shares a secret input among several parties, ensuring each share is verifiable. Motivated by its applications in the blockchain space, we focus on a VSS where parties holding shares are not allowed to reconstruct the dealer's secret (even partially) on their own terms, which we address as privacy-targeted collusion if attempted. In this context, our work investigates mechanisms deterring such collusion in VSS among rational and malicious parties. For this problem, we make both algorithmic and combinatorial contributions: 1. We provide two collusion-deterrent mechanisms to discourage parties from colluding and recovering the dealer's secret. Notably, when it is desired to achieve fairness---where non-colluding parties are not at a loss---while allowing for the best achievable malicious fault tolerance, we define ``trackable access structures'' (TAS) and design a deterrence mechanism tailored for VSS on these structures. 2. We estimate the size of the optimal TAS, construct them from Steiner systems, provide highly robust TAS using partial Steiner systems, and present efficient secret sharing schemes for the latter close-to-optimal TAS for various parameter regimes. 3. We demonstrate that trackability in access structures is connected to combinatorial objects like (partial) Steiner systems, uniform subsets with restricted intersections, and appropriate binary codes. The robustness of access structures is equivalent to the minimum vertex cover of hypergraphs. We believe these connections between cryptography, game theory, and discrete mathematics will be of broader interest.

NAT10 drives brain metastasis by regulating the serine synthesis pathway

Peng Xu

With Jocelyn F. Chen, Wesley L. Cai, Huacui Chen, Wenxue Li, Amer Balabaki, Ethan D. Krop, Elianna Asare, Yansheng Liu, Don X. Nguyen, Qin Yan

Metastasis is the major cause of cancer-related deaths. Emerging evidence has shown that epigenetic regulation plays a fundamental role in cancer metastasis. Here, we conducted an in vivo shRNA screen for vulnerabilities of brain metastasis and identified N-acetyltransferase 10 (NAT10), a multi-domain-and-functional protein, as a driver of brain metastasis. We showed that both its RNA helicase and N-acetyltransferase domains are essential for primary tumor growth and brain metastasis in vivo. Integrative transcriptomic and proteomic analyses revealed key downstream effectors of NAT10, including PHGDH and PSAT1, two catalyzing enzymes for serine biosynthesis implicated in brain metastasis. Distant metastases of breast cancer, especially brain metastases, express higher levels of NAT10, PHGDH, and PSAT1. Silencing PHGDH/PSAT1 in metastatic breast cancer cells inhibits their ability to grow in the serine/glycine-limited condition, phenocopying the effects of NAT10 depletion. Moreover, NAT10 promotes the expression of PHGDH and PSAT1 in its RNA helicase-dependent manner. These findings establish NAT10 as a key regulator of brain metastasis and nominate NAT10 and the serine synthesis pathway as potential targets for treating brain metastasis.

Acknowledgments:Note: Peng Xu and Jocelyn F Chen contributed equally. Wesley L Cai and Huacui Chen contributed equally as co-second authors

Molecular Networks in Silicosis: Transcriptomics Analysis in Exposure driven Pulmonary Fibrosis

Nebal Abu Hussein

With Nebal S. Abu Hussein, Taylor Adams, Sabina Anderson, Mordechai R. Kramer, Fadi Nikola, Robert Homer, Abderrahman Najjar, Prapti Sharma, Luning Yang, Yuening Zhang, Xiting Yan, Barak Pertzov, and Naftali Kaminski

Silica dust-induced pulmonary fibrosis is the most common occupational lung disease worldwide, and despite efforts at prevention is on the rise. While there has been substantial progress in studying animal models of silicosis, a detailed molecular understanding of the disease in humans is missing. Here, we combine bulk mRNA sequencing and spatial transcriptomics to identify the molecular and cellular networks underlying human end-stage silicosis. methods: 53 FFPE lung-samples were obtained from 27 explant endstage fibrotic silica patients who were exposed to artificial silica dust, and 28 healthy controls. RNA was extracted, and bulk RNA sequencing was performed. For Spatial transcriptomics, a tissue microarray with 24 different samples of 2mm each was constructed (14 Silica samples, 6 IPFs, and 4 controls) then we performed a spatial transcriptomics analysis using CosMx Spatial Molecular Imager. Data analysis was conducted using R with DESeq2 and EdgeR packages, and pathway analysis was conducted using Metacore. We used the Atomx platform and R packages for data integration and analysis for the Spatial analysis. Results: 26,485 genes were detected; after filtering out lowexpressed genes, we focused on 22,838 genes. Comparing the 53 silica samples to 28 controls using the DESeq2 method, 5735 genes were increased compared to controls, and 630 genes were decreased in silicosis lungs compared to controls (FDR<0.05 fold-change > 2 or <0.5 respectively). Among the increased genes were CTHRC1, COL1A1, COL3A1, matrix metalloprotease genes MMP1, MMP3, MMP9, MMP11, MMP12, MMP13, as well as markers of profibrotic macrophages such as SPP1, CHIT1, CHI3L1, MERTK among others. Using Spatial technology, we detected up to 1000 genes per Field of view. By integrating all the samples together, we identified all main compartments of the lung, including airways, capillaries, endothelium (arterial and venous), immune, and alveolar, with distinct changes in cellular and

gene expression patterns in silicosis lungs. Conclusions: The findings from our Bulk RNA Seq analysis and spatial transcriptomics provide the first in-depth molecular and cellular profile of advanced silicosis, with details about the extensive tissue remodeling characteristic of this devastating condition. This profile should be useful for generating novel hypotheses, biomarkers, and targets for therapeutic interventions.

Molecular insights into de novo small molecule recognition by an intron RNA structure

Ling Xu

With Tianshuo Liu, Kevin Chung, Luke Sisto, Jimin Hwang, Chengxin Zhang, Anna Marie Pyle

Targeting RNA with small molecules has become an appealing drug development strategy as it bears the promise of significantly expanding the druggable genome, making possible pharmacological targeting of genes that are either non-coding or difficult to target on the protein level. However, the identification of functionally active RNA binders faces low hit rates in routine chemical space exploration and lacks robust high-throughput screening assays. The visualization of atomic details of RNA-small molecule interactions also poses a challenge due to the dynamic nature of RNA molecules. To address these challenges, we leveraged high-throughput screening by establishing a molecular beacon-based platform, medicinal chemistry and structural biology to identify a de novo splicing inhibitor against a large and highly folded fungal group I intron from Candida Albicans. The high-resolution cryoEM structures of the intron RNA in different liganded states not only reveal molecular interactions that rationalize experimental structure-activity relationship, but also shed light on a unique strategy whereby RNA-associated metal ions and RNA conformation exhibit exceptional plasticity in response to small molecule binding. Our study reveals general principles that govern RNA-ligand recognition, the interplay between chemical bonding specificity, and dynamic responses within an RNA target, which offers valuable perspectives for RNA-targeted drug development.

Impact of LKB1 co-mutation in lung cancer on the functionality of antitumor T cells

Kelli Connolly

With Emily Borr, Dylan Mariuzza, Brittany Fitzgerald, Nikhil Joshi

Checkpoint inhibitor (CPI)-treated lung adenocarcinoma (LUAD) patients have seen unexpected survival benefits over the last decade, but response rates remain low and vary with certain genetic comutations. Notably, patients bearing comutations in KRAS and LKB1 (KL) are less responsive to CPI than patients with KRAS and P53 (KP) comutations and mechanisms have not been fully elucidated. Previously, we identified a reservoir of stem-like CD8 T cells, which mediate the response to CPI, that is maintained in the tumor-draining lymph node (tdLN), and that sustains the intratumoral population of therapy-responsive TCF+ CD8 T cells by migration. We hypothesize that tdLN reservoirs exist in both KP and KL tumors, but that signals received upon entry into tumors render these T cells unable to exert effector functions. A lack of appropriate mouse models has made it difficult to assess the direct impacts of these mutations on tumor-specific CD8 T cells. To test this directly, we generated genetically engineered mice harboring mutant Kras-G12D along with P53 and/or LKB1 deletion in autochthonous lung tumors sharing the same inducible neoantigen. Intriguingly, while tumor specific T cells are maintained similarly within tdLN in vivo and have comparable functional potential ex vivo, tumor-specific T cells are incapable of killing neoantigen+ LKB1-/- tumor cells in in vitro killing assays despite similar MHCI expression on LKB1-/- and LKB1+/+ tumor cells. These data suggest that KL tumors establish and maintain a tumor-specific, CPI-responsive CD8+ T cell response, but that these T cells are incapacitated by T cell-extrinsic

signals within KL tumors and/or a defect in recognition of tumor cell peptide-MHC. Single cell-RNA-sequencing of T cells support the latter, as expression of genes downstream of TCR signaling are decreased in T cells from KL compared to KP tumors. To test this, we will leverage RNAseq results from of KP and KL tumor cells to determine differentially expressed genes. These data will inform a series of in vivo assays in which neoantigen-inducible KL and KP LUAD organoids, generated from these mice, are edited in vitro, grown orthotopically, and T cell recognition and killing of tumor cells is read out via FACs analysis of Nur77-reporter T cells and %neoantigen-expressing/total tumor cells. Ultimately, this work will help to inform novel therapeutic strategies for CPI-refractory KL LUAD.

Dissecting the ancestry-specific genetic architecture of alcohol consumption in Latin American Individuals

José Martínez-Magaña

With Diego E. Andrade Brito1,2, Eirini Trichia3, Melody Rivera-Hernández1,2, Rachel L. Kember4,5, Diana L. Núñez-Ríos1,2, Jason Torres3, Roseann E Peterson6,7, Hang Zhou1,2, Jesús Alegre8, Jaime Berumen8, Pablo Kuri-Morales9,10, Roberto Tapia-Conyer9, Jonathan Emberson3, Henry R. Kranzler4,5, Amy C. Justice2,11,12,, Joel Gelernter1,2, Sandra Sanchez-Roige13,14,15, Sylvia Wassertheil-Smoller16, Krista M. Perreira17, Martha Daviglus18, Humberto Nicolini19, Alma Delia Genis-Mendoza19, Jorge Ameth Villatoro-Velazquez20, Maria Elena Medina-Mora20,21, Marycarmen Noemí Bustos-Gamiño20, Sintia Iole Belangero22.23, Marcos Leite Santoro22,23, Luis Augusto Rohde24,25, Rodrigo Affonseca Bressan24,26, Euripedes Constantino Miguel24,27, Pedro Mario Pan24,26,, Giovanni Abrahao Salum24,28,29, Katherine L. Tucker30, Jose M. Ordovas31, Dawn K. Coletta32,33, Oscar D Parra32, Yann C. Klimentidis34, Lawrence J. Mandarino32,33, Mariana Moysés-Oliveira35, Priscila F. Tempaku35, Monica L. Andersen35,36, Sergio Tufik35,36, Eva E. Lancaster37, Madhurbain Singh38, María Teresa Tusié-Luna39,40, Carlos A. Aguilar-Salinas41, Ana Ochoa-Guzmán42, Alexandre Pereira43, Karen G. Martinez-Gonzalez44, 23andMe Inc Research Team, Latin American Genomics Consortium, S4S Working Group, Elizabeth G. Atkinson45,46, Paola Giusti-Rodríguez47, Janitza Montalvo-Ortiz1,2,*

Genome-wide association studies (GWAS) have made substantial contributions to our understanding of the genetic liability of alcohol consumption. However, the diversity of populations included in large-scale GWAS is suboptimal, with Latin American populations representing around 1.79% among those with the lowest representation. The Latin American (LA) population is remarkably diverse, being an admixture of genomic segments from several ancestries. These admixture creates a challenge in modeling the genetic architecture of complex traits. Recent advancements have introduced innovative techniques using local ancestry data, the information of the ancestral origin of the genetic variant, to overcome this challenge. In this study, led by members from the Latin American Genomics Consortium (LAGC), we conducted a large-scale meta-analysis of GWAS studies of self-reported alcohol consumption in 465,516 individuals from cohorts based in Latin American countries and the United States (US); and also conducted local ancestry-aware GWAS on 11,655 LA individuals, substantially expanding the representation of Latin American and Caribbean populations. In the large-scale GWAS, we replicated well-known genetic associations for alcohol consumption in genes like CADM2 and the ADH's loci. Also, we found a signal in the ALDH2 locus, a previous association only found in Asian populations. We also identified heterogeneity in the transferability of polygenic scores across the geographically diverse Latin American subgroups. Using the novel ancestry-aware GWAS, we identified associations with rs1874323 (p-value = 2.5760e-08) in the MAGI1 gene, rs6833926 (p-value = 3.0010e-08) in the ARAP2 gene, two in the

SLIT3 gene (rs73805262, p-value = 9.9540e-09; rs115143510; z = p-value = 1.2250e-08), and one intergenic variant (rs3929849, p-value = 2.3930e-09) in those individuals where the section of the genome comes from AFR descent. We also identified associations in intergenic variants in those where the region is of AMR descent (rs4130378, p-value = 9.673e-09; rs536315876 p-value = 4.3640e-09; rs115675116, p-value = 4.3190e-09). Our study adds to current efforts to elucidate the genetic architecture of alcohol consumption in Latin American populations and implicates novel genes for further research. The novel genetic associations identified in admixed Latin American individuals highlight the importance of conducting local ancestry-aware GWAS to identify potential ancestry-specific loci.

Acknowledgments:JJMM was supported by NIDA R21DA050160 and DP1DA058737. JJMM was also supported by the Kavli Postdoctoral Award for Academic Diversity.

Access to Chronic Non-Communicable Disease Medications During Wartime in Sudan

Eman Salih

With Kaveh Khoshnood; Saria Hassan; Faihaa Dafalla; Amina Hassan, Amin Abdellatif; Ahmed Elzamzami

Sudan's protracted conflict has significantly disrupted the national health system, deepening barriers to essential health services and placing patients with chronic non-communicable diseases (NCDs) at heightened risk. This qualitative study explores the systemic challenges and emergent local solutions related to the availability, accessibility, and affordability of chronic disease medications in the context of conflict. Drawing on interviews with key stakeholders—including national health authorities, international partners, and diaspora organizations—alongside media analysis and literature review, this research presents a timely examination of governance, supply chain disruption, and adaptive responses within Sudan's evolving health landscape. Preliminary findings highlight the impact of warehouse occupation, security threats, and economic deterioration on NCD medication access, while also documenting local innovations ranging from informal distribution mechanisms to transnational collaborations that aim to safeguard continuity of care. By situating the Sudanese case within broader humanitarian and health systems discourses, this study offers practical insights for policymakers, donors, and global health actors committed to ensuring equitable access to chronic disease care in fragile and conflict-affected settings. It underscores the importance of context-specific strategies, systems thinking, and cross-sectoral coordination in advancing health equity amidst crisis.

A comparative analysis of protein interactors of Kv1.3 in Microglia and T-Cells: Implications for Neurodegenerative and Autoimmune Diseases

Dilpreet Kour

With Christine A. Bowen, Upasna Srivastava, Hai M. Nguyen, Rashmi Kumari, Prateek Kumar, Heike Wulff, Nicholas T. Seyfried, Srikant Rangaraju

The voltage-activated Kv1.3 potassium channel is expressed in brain resident and peripheral immune cells. Kv1.3 functionally couples with key immune proteins to regulate immune signaling, particularly microglia-mediated neuroinflammation and T cell-mediated autoimmunity. To identify cell-type-specific and disease-associated interactors of the Kv1.3 channel, we employed TurboID-based proximity labeling and characterized the interactomes of Kv1.3 in microglia and T-cells. We generated Kv1.3-expressing BV2 microglia and Jurkat T-cells and used mass spectrometry proteomics of labeled proteins to identify

863 interactors of Kv1.3 in microglia and 1845 interactors in T-cells. Microglia-specific Kv1.3 interactors primarily function in energy and lipid metabolism, while T-cell-specific Kv1.3 interactors regulate cell signaling and protein phosphorylation. We also identified 280 and 335 cell surface proteins in the Kv1.3 interactome in microglia and T-cells, respectively. While 12 of the plasma membrane interactors were common (e.g. ITGB1, STOM), none of the mitochondrial membrane interactors were shared across microglia and T-cells. Importantly, we identified 293 disease-relevant interactors of Kv1.3, including 82 Alzheimer's disease (AD)- and 39 Parkinson's disease (PD)-associated genes in the microglial interactome, as well as 178 autoimmune disease-associated genes in the T-cell interactome. These disease interactors function primarily in signaling receptor (AD), antigen processing (PD) and immune signaling (autoimmunity). Infiltrated T-cells in AD brain contribute to neurodegeneration, while the association of T-cell' Kv1.3 in this is unknown. To identify Kv1.3-associated pathways that are perturbed by Kv1.3 blockade in AD, we used ShK-223 (for 3mo, i.p.) to block Kv1.3 channels in a 5xFAD model (6mo) and analyzed bulk mRNA seq from brain. Kv1.3 blockade differentially impacted ~900 Kv1.3 interactors (431 Up and 468 Down). Kv1.3 blockade affected cholesterol/lipid metabolism genes identified from microglial interactome, and PI3K signaling and RNA metabolism genes from T-cells interactome. Among the disease-relevant interactors of Kv1.3, Shk-223 treatment upregulated genes involved in the regulation of immune processes, while many ER- and Golgi-specific genes were downregulated. Overall, the Kv1.3 interactomes in microglia and T-cells highlight the specialized functions of the channel, tailored to neuroinflammatory regulation in microglia and immune response modulation in T-cells. The insights gained from this research further emphasize the role of Kv1.3 channel in immunomodulation and provides a framework for future cell type-specific mechanistic studies to explore Kv1.3 channels as therapeutic targets for neuroinflammatory and autoimmune diseases.

Preclinical efficacy of the estrogen receptor degrader fulvestrant in combination with RAF/MEK clamp avutometinib and FAK inhibitor in low-grade serous ovarian cancer with acquired resistance to chemotherapy and aromatase Inhibitor

Cem Demirkiran

With Stefania Bellone, Victoria Ettorre, Tobias Max Philipp Hartwich, Michelle Greenman, Blair McNamara, Yang Yang-Hartwich, Elena Ratner, Peter E. Schwartz, Silvia Coma, Jonathan A. Pachter, Alessandro D. Santin

Objectives. Low-grade serous ovarian carcinomas (LGSOC) are rare ovarian tumors characterized by a high recurrence rate and limited treatment options. LGSOC are frequently estrogen receptor/progesterone receptor (ER/PR) positive and activating mutations in KRAS (~30%), NRAS (~10%), and BRAF (~8%) are critical to the pathogenesis of LGSOC. These molecular features have important implications for the targeted treatment of LGSOC. Avutometinib is a dual RAF/MEK inhibitor, whereas defactinib and VS-4718 are inhibitors of focal adhesion kinase (FAK). Fulvestrant is an estrogen receptor antagonist/degrader and was used as representative of various antiestrogen approaches including aromatase inhibitors. We assessed the preclinical efficacy of fulvestrant single agent, avutometinib + VS-4718 (FAKi), and the triple combination in LGSOC patient-derived tumor xenografts (PDX). Methods. Tissue obtained from a LGSOC patient wild-type for KRAS/NRAS/BRAF mutations whose disease progressed after chemotherapy and anastrozole was transplanted into female CB17/lcrHsd-Prkdc/SCID mice as PDX (OVA(K)250). The animals were treated with either saline/control, fulvestrant, avutometinib/FAKi, or the triple combination of avutometinib/FAKi/fulvestrant for 32 days. Avutometinib and FAKi were given five days on and two

days off through oral gavage. Fulvestrant was administered subcutaneously once a week. Mechanistic studies were performed ex vivo using western blot assays. Results. Animals treated with the triple combination of avutometinib/FAKi/fulvestrant demonstrated stronger tumor-growth inhibition compared to all the other experimental groups tested including control/saline ($p < 0.001$), single agent fulvestrant ($p = 0.04$ from day eight and onwards), and avutometinib/FAKi ($p = 0.02$ from day 18) (Figure A). Median survival for mice treated with saline/control was 29 days while all the mice in other experimental groups were alive at day 60 ($p < 0.0001$ and Figure B). Treatment was well tolerated across all experimental groups. By western-blot assays, exposure of OVA(K)250 to the triple combination demonstrated a decrease in phosphorylated FAK (p-FAK) and p-ERK expression. Conclusion. Addition of avutometinib/FAKi to fulvestrant enhances in vivo activity of fulvestrant in LGSOC-PDX with acquired resistance to chemotherapy and aromatase inhibitors and the triplet combination was well tolerated.

Artificial Intelligence Enhanced Cardiovascular Disease Prediction using Electrocardiogram Images

Bruno Batinica

With Dhruva Biswas, Lovedeep Dhingra, Arya Aminorroaya, Evangelos Oikonomou, Rohan Khera

Accurate quantification of cardiovascular disease (CVD) risk is essential for guiding treatment initiation decisions. Traditional risk equations often leave a substantial intermediate-risk group wherein decision-making regarding preventive therapy is uncertain. Methods: We developed a time-to-event vision transformer neural network (ECG-CVD) to predict incident CVD directly from raw electrocardiogram (ECG) images. The model was trained on digital ECGs from 404,321 adults aged 30–75 years without prior CVD at Yale, with a median follow-up of 4.9 years. Model performance was internally evaluated via fivefold cross-validation and external validation was conducted in the UK Biobank. Results: In the derivation cohort, ECG-CVD achieved a concordance index (C-index) of 0.75 (95% CI: 0.73–0.76). In the UK Biobank, it attained a C-index of 0.70 (95% CI: 0.66–0.74), outperforming PREVENT-alone (C-index 0.68, $p < 0.01$). Among participants classified as intermediate risk by PREVENT, ECG-CVD score yielded significantly separated Kaplan Meier survival curves (log-rank $p < 0.001$). Predictions remained stable across repeat ECGs (intraclass correlation coefficient = 0.85) and when using single-lead (lead I) waveforms (C-index = 0.74). Conclusions: We demonstrate that ECG-based deep learning can refine CVD risk stratification. This approach holds promise for noninvasive, scalable CVD risk assessment, guiding earlier preventive interventions.

Sex-Based Disparities in Thoracic Aortic Disease

Afsheen Nasir, MD

With Christina Waldron, BS; Ely Erez, MD; Hiren Parekh; Abdulrahman Hassab, MD; Argyrios Gyftopoulos, MD2; Kristina Wang, BS; Alan Chou, MD1;; Prasanth Vallabhajosyula, MD; Karthik Murugiah, MD; Roland Assi, MD, MMS

1. Sex-Based Outcomes of Elective Proximal Thoracic Aortic Aneurysm Surgery Introduction: The effect of sex on the outcomes of thoracic aortic surgery is not well known. We report our aortic center's outcomes of elective proximal thoracic aortic surgery by sex. Methods: Electronic health records of all patients undergoing elective root and/or ascending aortic aneurysm replacement between 2017 and 2022 were reviewed. Information regarding demographics, comorbidities, intervention, and postoperative

course including major adverse cardiovascular events (MACE) was extracted for patients. Data were compared between male and female patients using chi-square tests and fisher exact tests for categorical variables, and t-test for continuous variables. Survival and associates of worse early outcomes were analyzed using Kaplan Meier analysis and multivariate logistic regression. Results: 574 patients underwent elective aortic surgery between 2017 and 2022. 74.7% were male (429/574) and 25.3% were female (145/574). Average follow-up was 4.2 ±1.7 years. Women were older at the time of surgery compared to men (64 ±13 vs 61.4 ±11.9 years, p=0.03). Men had a greater body surface area compared to female patients (21.2±0.2 vs 1.81±0.23 m2, p<0.001). There were no statistically significant differences in baseline comorbidities between groups, except diabetes mellitus which had a higher prevalence in men (15.9% vs 8.3%, p=0.03). Women had larger, although statistically insignificant, aortic surface to height ratio compared to male patients (9.96 ±2.66 vs 10.5 ±3.28, p=0.08) at the time of surgery, more operations involving the ascending aorta (91.7% vs 76.2%, p<0.001), and less operations involving aortic root (28.3% vs 50.6%, p<0.001). Men had more concomitant coronary artery bypass surgeries (14% to 5.5%, p=0.01), significantly longer surgeries (359 vs 326 min, p=0.002), as well as cardiopulmonary bypass (193 vs 162 min, p<0.001) and cross-clamp times (144 vs 110 min, p<0.001) compared to women. Operative mortality was higher for women (0.2% vs 2.1%, p=0.05). Mortality at follow-up was higher for women (3.96% vs 8.28%, p=0.04). Postoperative (30-day) complications were higher in women for the following conditions: permanent stroke (2.1% vs 0.2%, p=0.05), postoperative bleeding (5.5% vs 2.1%, p= 0.04) and pleural effusions requiring drainage (8.3% vs 2.8%, p<0.001). Conclusions: At the time of elective proximal thoracic aortic surgery, women were older and had larger aortic surface to height index compared to men. Women had worse postoperative survival, postoperative morbidity, and mid-term survival compared to men. 2. Sex-based Characteristics of Clinical Presentation and Surgical Outcomes of Type A Aortic Dissection Repair Introduction: Studies have shown delayed presentation of women with acute aortic events and worse surgical outcomes compared to men. We report our aortic center's experience with the clinical presentation and surgical outcomes of acute type A aortic dissection by sex. Methods: Electronic health records of all patients undergoing type A dissection repair between 2017 and 2022 were reviewed. Data were compared between male and female patients using chi-square and fisher exact tests for categorical variables, and t-test for continuous variables. Results: Of the 135 patients, 67% were male (90/135) and 33% female (45/135). Women were older in age (67.9 vs 60.5 years, p = 0.004), had smaller height, weight, and BSA (162.2 vs 177.8 cm, p <0.001; 75.3 vs 97.3 kg, p<0.001; 1.79 vs 2.13 m2, p<0.001). Twenty-nine percent men vs 15.6% women had a known diagnosis of thoracic aortic aneurysm, p=0.13. All baseline comorbidities were similar between the groups, except cerebrovascular disease that was more prevalent in men, 0% vs 11.1%, p=0.03. Upon presentation, Penn class A, B, and C malperfusion was noted in 37.8% (34/90), 26.7% (24/90) and 35.5% (32/90) male, and 37.8% (17/45), 24.4% (11/45), 37.8% (17/45) female patients (p=1, p=0.91, p=0.75). No statistically significant difference was observed in the clinical presentation of chest pain, neurological deficit, cardiogenic shock, hemopericardium, dissection rupture, and valve pathologies. Location of primary tears in the aorta, as well as retrograde and antegrade extension were similar in both groups. Women had more procedures involving hemiarch repair 88.9% (40/45) vs 70% (63/90), p=0.01; total arch was repaired more often in men 8.9% (4/45) vs 23.3%, (21/90) p=0.04. Antegrade cerebral perfusion was more often utilized in men, 17.8% (8/45) vs 38.9% (35/90), p=0.01, while retrograde cerebral perfusion was more commonly used in women 55.5% (25/45) vs 30% (27/90), p=0.004. All other perioperative parameters were comparable. Stroke 6.7% vs 11.1%, p=0.5, renal failure requiring dialysis 11.1% vs 20%, p=0.29, deep sternal wound infection 4.4% vs 3.3%, p=1, reoperation 6.7% vs 10%, p=0.75 were

similar across the groups, among other postoperative complications. Thirty-day or in-hospital mortality was 6.7% vs 15.5%, p=0.17, and 1-year mortality beyond initial 30-days was 6.7% vs 4.4%, p=0.68, among female and male patients. Conclusions: No difference was noted in the clinical presentation of type A aortic dissection, as well as in the post-operative course and survival after repair. 3. Sex-Based Patterns Of Imaging Surveillance And Follow-Up In Patients With Ascending Thoracic Aortic Disease Introduction We aim to evaluate whether a sex-based disparity exists in the patterns of thoracic aortic aneurysm surveillance and management. Methods: Echocardiograms between 2017 and 2022 at a single healthcare system were extracted for patients with sinus of Valsalva or ascending aorta ≥4 cm. Data on aortic specialists referral and imaging surveillance within 6-18 months were collected. Results: A total of 540,852 echocardiographies were done for 262,098 patients (125,535 males, 136,563 females).12.3% (20.7% males; 4.5% females) of all patients were found to have dilated sinus of Valsalva or ascending aorta on routine imaging, of which 80.9% were male (average age 73.2 years) and 19.1% were female (average age 75.6 years). Overall, 73.9% of patients (74.3% males, 72.4% females, p=0.003) had an appropriate follow up imaging or cardiovascular medicine (CVM) or cardiothoracic surgery (CTS) referral in place. Of the 81.3% patients (81.3% males, 81.3% females, p=1) who underwent surveillance echocardiography or chest CT imaging, 46.9% (46.8% males, 47.4% females, p=0.5) were imaged within 6-18 months of the index study. Overall, 63.3% patients (63.9% males, 60.9% females, p<0.001) had a CVM (63%; 63.6% males, 60.5% females, p<0.001) or CTS (3.1%; 3% males, 3.6% females, p=0.04) referral in place. 70.2% of new CVM referrals (70.4% males, 69.7% females, p=0.7) and 55.7% new CTS referrals (54.4% males, 60% females, p=0.2) were placed within 18 months of index study. Conclusion: While surveillance imaging for patients with proximal aortic dilation was similar, women had a lower rate of referral to cardiology and higher rate of referral to cardiac surgery. 4. Pregnancy-associated Vascular Complications and Thoracic Aortic Growth Patterns Introduction: Pregnancy induces hemodynamic stress that may predispose the thoracic aorta to accelerated growth or acute events. Here we present a single center experience with vascular outcomes in the obstetric population with thoracic aortic disease. Methods: Electronic health records of pregnant patients with thoracic aortic aneurysm at our healthcare system were reviewed. Information was collected regarding demographics, aortic size, arterial complications, and clinical management of pregnancy. Results: Twenty-six patients with a total of 92 pregnancies (median per patient=3, IQR 2-4) were identified. Data were available for 39 pregnancies between 2011 and 2023. At the time of the first pregnancy, 23% (6/26) patients had no known diagnosis of thoracic aortic aneurysm despite 2 patients known to have connective tissue disease. 57.7% (15/26) patients had a heritable cause of TAD. 42.3% (11/26) had no known underlying cause, hence labelled as sporadic dilations. 11.5% (3/26) suffered vascular complications in association with pregnancy. All vascular complications occurred in patient with heritable TAD. No type A aortic dissection was noted. Aortic surveillance and imaging schedule were variable among patients. Conclusions: Proximal aortic growth pattern is variable across pregnancy. No acute aortic events were observed during pregnancy. However, risk of pregnancy-related vascular complications is higher during postpartum period.

Selected Lightning Round Talks

Increasing Trends of Polysubstance Use among Lesbian and Bisexual US Female Adults

Luis Mestre

With Juhan Lee, Maria A. Parker, Marney A. White, & Krysten W. Bold

Introduction: The substance use crisis in the US is worsening, particularly among lesbian, gay, and bisexual (LGB) female adults which are more likely to engage in this behavior. Understanding recent trends of this behavior is essential to make decisions about how to mitigate the exacerbated risks among LGB adults in this crisis. We aim to assess the trends of polysubstance use prevalence among LGB adults in the US by sex . Methods: We analyzed the National Survey on Drug Use and Health dataset of US adults from 2021 to 2023 (age 18+; n=127,645). The outcome, polysubstance use, was defined as using two or more substances past 30 days. The exposure was sexual identity. Linear and quadratic trend tests for polysubstance use prevalence were conducted to measure differences by sexual identity and sex over time, adjusted by sociodemographic factors. Results: Both lesbian (coef = 0.12; p <0.001) and bisexual (coef = 0.07; p <0.001) female adults had a linear increasing trend in their polysubstance use prevalence from 2021 to 2023. Lesbian female adults had the highest increasing change of polysubstance use prevalence from 2021 to 2023 (17.27%; p <0.001), followed by bisexual female adults (10.60%; p<0.001). Conclusion: LGB female adults had the fastest increasing trends among all groups by sexual identity and sex from 2021 to 2023. Providing additional resources to develop effective strategies that address polysubstance use among LGB female adults may help mitigate the risk of the substance use crisis in the US worsening.

Collective intelligence of specialized language models guides de novo chemical synthesis

Sumon Sarkar

With Haote Li, Wenxin Lu, Patrick Loftus, Tianyin Qiu, Yu Shee, Abbigayle Cuomo, John-Paul Webster, H. Ray Kelly, Vidhyadhar Manee, Sanil Sreekumar, Frederic Buono, Robert Crabtree, Timothy Newhouse, and Victor Batista.

Harnessing the vast and expanding repository of synthetic knowledge remains a fundamental challenge in modern organic chemistry. While recent application of large language models (LLMs) has demonstrated potential, their effectiveness in predicting de novo chemical synthesis remains limited. Here, we introduce MOSAIC (Multiple Optimized Specialists for AI-Driven Chemical Prediction), a computational framework that leverages the collective intelligence of millions of reaction protocols to generate reproducible, human-readable synthetic procedures. Built on the open-source Llama3.1-8B-instruct architecture, MOSAIC employs 2,489 specialized models trained on Voronoi-clustered reaction spaces to deliver high-precision predictions for complex organic transformations. Experimental validation confirms MOSAIC's predictive accuracy and practical utility across diverse reaction classes, including Buchwald-Hartwig amination, Suzuki coupling, and olefin metathesis. The successful synthesis of over 35 novel compounds spanning pharmaceuticals, materials, agrochemicals, and cosmetics underscores its broad applicability. Notably, MOSAIC's potential to guide the development of new synthetic methods has been demonstrated, highlighting its significant impact on chemical synthesis. By redefining the interface between artificial intelligence and experimental chemistry, MOSAIC provides a scalable and interpretable approach to accelerating chemical innovation.

Acknowledgments:Yale University, Boehringer Ingelheim, National Science Foundation

Adoptive Transfer of Preeclampsia-Exposed T Cells Increases Blood Pressure and Arterial Stiffness Without Microvascular Alterations Following Repeated Hypertensive Stimuli in Female Mice

Michele D'Agata

With Michele N. D'Agata, Pretty S. Joy, Olivia Monte, Lauren A. Biwer

Preeclampsia (PE) is new-onset hypertension with major organ damage after 20 weeks of gestation. Although overt PE signs resolve after placental delivery, postpartum microvascular dysfunction and increased future hypertension risk are evident. PE increases circulating T cells and adoptive transfer of placental T cells from PE cases to pregnant nude athymic rats results in hypertension. T cells may promote hypertension through vascular alterations, however, whether PE-exposed T cells induce microvascular dysfunction and hypersensitivity to hypertensive stimuli is unknown. We hypothesize that transferring PE-exposed T cells to T cell-deficient (TCRα-/-) female mice increases blood pressure, arterial stiffness, and microvascular dysfunction following repeated hypertensive stimuli compared to normal pregnant (control) T cells. T cells isolated from spleens and iliac lymph nodes of PE (sFlt1 adenovirus) or control (CMV-null adenovirus) pregnant mice were adoptively transferred to T cell-deficient female mice. Six weeks post-transfer, mice were administered high dietary sodium followed by AngII infusion. Blood pressure (telemetry), aortic stiffness (pulse wave velocity), and microvascular function (mesenteric arteries excised for wire myography) were assessed post-stimuli. Groups were compared using independent T tests. Data are reported as mean ± SEM. Compared to control T cell recipients (2-3 mice/experiment), PE T cell recipients (3-4 mice/experiment) had higher systolic blood pressure (PE: 157±2, Control: 121±2, mmHg; P=0.001) and aortic stiffness (PE: 5.1±0.6, Control: 3.3±0.2, mm/ms; P=0.05). Microvascular function (acetylcholine-induced relaxation) was not different between groups (P=0.22). PE-exposed T cells induced hypersensitivity to future hypertensive stimuli independent of alterations in microvascular function, thus other mechanistic pathways should be considered.

Acknowledgments:Funding: NIH-NHLBI K99/R00 HL161321. We also acknowledge assistance and scientific expertise from personnel from the following Yale laboratories: Fernandez-Hernando, Suarez, Libreros, and Raredon.

Endothelial-specific LRP5 deletion mitigates atherosclerosis

Rizwana Afroz

With Begoña Lainez-Mas, Julie E. Goodwin

Atherosclerosis is a common pathologic condition and a major cause of progressive cardiovascular disease. Cellular signaling pathways play a pivotal role in the development of atherosclerosis, emerging evidence indicates the involvement of the Wnt signaling in this process. Suppressing canonical Wnt signaling can improve the atherosclerotic phenotype. Since endothelial dysfunction is an early hallmark of atherosclerosis, endothelial-specific Wnt inhibition may offer protection against the disease. To evaluate the mechanistic contribution of Wnt signaling in atherosclerosis progression, a novel mouse model was utilized. We have targeted the key co-receptors in the Wnt signaling network: low-density lipoprotein receptor-related protein 5 (Lrp5) and Lrp6, and generated mice that lack endothelial specific Lrp5 or Lrp6. These mice were subsequently bred onto an ApoE knockout (ApoE−/−) background. In this study, we showed that endothelial-specific deletion of Lrp5 led to reduced arterial lipid deposition and decreased atherosclerotic plaque size. Mechanistically, the lack of Lrp5 reduces the inflammation and release of pro-inflammatory cytokines. The findings of this study highlight the contribution of endothelial Wnt signaling in the progression of atherosclerosis, which could potentially facilitate new therapeutic advances in the treatment of the disease.

Brain-based prediction of gaming disorder in adolescents

Jennifer Park

With Cheryl Lacadie, Dustin Scheinost, Li Yan McCurdy, Yihong Zhao, Marc N. Potenza

Background: Gaming disorder (an addiction to video games) appears to be more prevalent among adolescents than adults. However, data-driven research to identify neural networks predictive of problematic gaming in adolescents remains limited. The aim of this study was to identify neural networks predictive of gaming disorder using connectome-based predictive modelling (CPM), a machine-learning approach that employs whole-brain functional connectivity data. We hypothesized that CPM would successfully predict gaming disorder scores in adolescents. Methods: The study analyzed data from the two-year follow-up of the Adolescent Brain Cognitive Development study (N = 1036, Mage = 12.0, SD = 0.6), when gaming disorder measures were introduced. CPM was applied to gaming disorder scores and functional magnetic resonance imaging (fMRI) data collected during the performance of a reward-processing task. Additional CPM analyses were conducted using resting-state and other task-based fMRI data relevant to response inhibition, emotion regulation, and working memory. Results: CPM successfully predicted gaming disorder scores. Highly predictive connections were observed within and between networks implicated in cognitive control and executive function (frontoparietal and medial frontal networks), visual processing (visual area 2 and visual association networks), and salience processing and motor response (salience and sensorimotor networks). CPM also predicted gaming disorder scores across all other analyzed brain states. Conclusion: Large-scale networks predictive of gaming disorder in adolescents were identified. These networks may be targeted in novel and personalized interventions, which may inform the development of treatment for gaming disorder.

Acknowledgments:This work was supported by the National Institute of Mental Health (RF1MH128614).

Role of GCC2 in T-cell mediated allograft rejection in mice

E M Tanvir

With John Pell, Anand Reghuvaran, Ashwani Kumar, Lingfeng Qin, Mandel-Brahm, George Tellides, Madhav C Menon

Non-HLA, donor-recipient (D-R). mismatches are recognized contributors to non-self responses and allograft failure. We used unbiased genetic and transcriptomic analyses to report the association of intronic and directional LIMS1 D-R mismatches. These SNPS regulate GCC2 a Golgin involved in endosome to golgi recycling of mannose-6-phosphate receptors (M6PR); however, the underlying mechanisms whether related to anti-LIMS1 antibodies or cell-mediated mechanisms are unclear, Here we characterized the immune phenotype of GCC2 knockout GCC2 (-/-) and GCC2 (+/-) [to mimic low-expressor SNPs] and C57BL/6J wildtype (WT) and performed aortic transplantation. GCC2 KO mice of both sexes had normal weight gain, and splenocyte counts compared to WT. In splenocyte FACS analysis, we identified that CD4+T- and B-cells, but not innate immune cells, had surface levels of M6PR proportionate to GCC2 gene dose. GCC2 KO and GCC2 (+/-) mice had significantly higher levels of activated CD4+CD44+CXCR3+, CD8+CD69+T cells and TCMs (CD4+CD44+CCR7+), similar levels of CD4+CD44+Tcells but significantly lower levels of Tregs (CD4+FoxP3+) and Th17 vs WT. Moreover, M6PR+FoxP3+cells were also significantly lower in GCC2 KO mice vs WT. Ex vivo, GCC2 KO mice generated significantly higher levels of CD4+ and CD8+CD44+ specific IL2 and TNFa compared to WT after PMA/ionomycin. In Treg polarizing conditions of TCR stimulation, GCC2 KO

CD4+T-cells proliferated more with the higher levels of Th1 markers but developed fewer Tregs. Simultaneously we evaluated IgG autoantibody profile using a PHIP-seq platform. Neither Anti-LIMS1 IgG or overall IgG autoantibodies were increased in GCC2 KO vs WT mice. We performed pilot aortic transplantation in a non-MHC mismatched context. Here, GCC2 KO mice showed significantly higher splenic CD4+CD44+T cells and CD4+KLRG1+T cells vs WT. Phenotypic characterization of graft rejection via new intima formation and T-cell infiltration is in progress. We report the role of GCC2 gene dose in mediating CD4+T-cell phenotype and Treg development, ascribing mechanism to directional LIMS1-SNP mismatches that clinically associate with kidney graft survival.

Association of Ptsd Symptom Trajectories with Accelerated pace of Epigenetic Aging in U.s. Military Veterans

Sheila Nagamatsu

With Robert H. Pietrzak, Ian C. Fischer, Joel Gelernter, Janitza Montalvo-Ortiz

Background: Mental disorders such as posttraumatic stress disorder (PTSD) are prevalent among U.S. military veterans. PTSD is often a chronic and disabling condition characterized by intrusive thoughts, avoidance, negative alterations in cognitions and mood, and heightened arousal and reactivity. It is associated with poor mental and physical health outcomes, as well as accelerated biological (i.e., epigenetic) aging, the latter of which may serve as a mechanism linking PTSD to adverse health effects and premature mortality. While numerous studies have demonstrated cross-sectional associations between PTSD and accelerated epigenetic aging, the longitudinal impact of PTSD symptom trajectories on the pace of epigenetic aging remains poorly understood. Methods We conducted a 10-year prospective study of 156 European American male U.S. military veterans and assessed PTSD symptoms at five time points over the study period. Saliva samples were collected at baseline and again at the 10-year follow-up for DNA methylation (DNAm) analysis. Epigenetic aging was estimated using the DNA Methylation Age Calculation for DNAm GrimAge2. PTSD symptom trajectories were identified using the "Traj" R package. The pace of epigenetic aging (PACE) was calculated as the difference in accelerated GrimAge2 between 2011 and 2021 (AccelGrimAge2021 - AccelGrimAge2011). Multivariable linear regression followed by a stepwise regression analyses were conducted to assess the relationship between PTSD symptom trajectories and PACE, adjusting for buccal cells CD4+ T cells, and monocytes. Additional cell types were removed to avoid multicollinearity. Results: Three distinct PTSD symptom trajectories emerged: stable/no change from baseline (N=48), increasing symptoms over time (N=36), and decreasing symptoms (N=10). A significant positive association was observed between the increasing PTSD symptom trajectory and GrimAge2 PACE (estimate=1.67,p=0.007), indicating that veterans with worsening PTSD symptoms over the 10-year period exhibited a more accelerated pace of biological aging relative to the stable condition. No significant association was identified for decreasing symptoms. Conclusion: Increases in PTSD symptoms over a 10-year period are associated with an accelerated pace of epigenetic aging in U.S. military veterans. These results underscore the biological toll of chronic stress and highlight the importance of early and sustained interventions for PTSD. Further research is needed to elucidate causal mechanisms and evaluate whether evidence-based treatments for PTSD mitigate accelerated epigenetic aging.

Tick-Tock: Tafenoquine vs. Malaria and Babesiosis.

Pratap Vydyam

With Anasuya C Pal, Isaline Renard, Meenal Chand , Vandana Kumari , Joseph C Gennaro , Choukri Ben Mamoun

Time races against human malaria and babesiosis, a tick-borne disease caused by intraerythrocytic protozoan parasites. As therapeutic resistance rises, novel pharmacotherapies are urgently needed. Tafenoquine, an 8-aminoquinoline antimalarial targeting malaria's hepatic hypnozoites, emerges as a dual-threat contender. We report its efficacy across protozoan parasites. In vitro, tafenoquine inhibits erythrocytic replication of Babesia spp.; in vivo, it potently suppresses parasitemia in murine models of Babesia microti and Babesia duncani, ensuring survival against lethal atovaquone-sensitive and -resistant B. duncani strains. Synergistic use with atovaquone achieves sterilizing immunity—complete parasite clearance without recrudescence—in both babesiosis models. Intriguingly, post-treatment clearance of B. duncani elicits robust adaptive immunity, protecting against rechallenge, akin to malaria prophylaxis. Cell biology studies reveal tafenoquine triggers cellular stress in parasites. Overall, this study unveils a molecular "tick-tock": a single agent dismantling two vector-borne threats. Tafenoquine offers transformative potential for malaria relapse prevention and babesiosis eradication through innovative pharmacodynamics and immunological priming, marking a breakthrough in parasitic disease control.

Acknowledgments:Blood donors and This work was supported by the National Institutes of Health (grant numbers AI123321, AI138139, AI152220, and AI136118); the Steven and Alexandra Cohen Foundation (grant number Lyme 62 2020); and the Global Lyme Alliance.

ROLE OF CFTR IN SGK1 AND STRESS-INDUCED SIGNALING IN MOUSE INTESTINE

Caroline Muiler Barbosa Nogueira

With Anderson K Santos, Parinaz Dastoor, Jason Jin, Diego C. dos Reis, Kazi Hoque, Nadia Ameen

Background: Cystic Fibrosis Transmembrane Conductance Regulator (CFTR) is regulated by phosphorylation and protein traffic. Pharmacologic inhibition implicated SGK1 signaling in regulating CFTR in rat intestine. To confirm the role of SGK1, we generated intestine-specific Vil1-Cre/SGK1 knock-out (KO) mice to examine the effect of acute stress on SGK1 signaling, CFTR expression, and ion transport. Methods: SGK1 mRNA expression was analyzed by qPCR and Semiquantitative RT-PCR (sqRT-PCR) in SGK1fl/wt and SGK1fl/fl mice vs WT mice. SGK1fl/wt and SGK1fl/fl mice were treated with dexamethasone (DEX) to activate the SGK1 pathway or PBS for 1 or 4 h. CFTR, total and phosphorylated SGK1 and NEDD4.2 were analyzed in tissue lysates by immunoblot. CFTR was examined in tissue sections by immunofluorescence (IF) localization and ion transport was analyzed by Ussing Chamber electrophysiology (UC). Results: qPCR and sqRT-PCR confirmed the absence of SGK1 expression in SGK1fl/fl and reduced levels in SGK1fl/wt compared to WT mice. Immunoblots confirmed the loss of SGK1 protein in SGK1fl/fl mice, while DEX-treated SGK1fl/wt mice exhibited increased SGK1, pSGK1, CFTR, NEDD4-2, and pNEDD4-2 protein levels, confirming SGK1 pathway activation. 1 h DEX-treated mice displayed higher SGK1 activation. CFTR levels were elevated in DEX-treated SGK1fl/fl mice, especially at 4h, an unexpected finding. qPCR and sqRT-PCR confirmed expression of SGK2 and SGK3 in SGK1fl/fl mice, suggesting compensation by these isoforms. IF analysis showed higher apical CFTR staining in crypts of 1 h DEX-treated SGK1fl/wt mice, consistent with enhanced CFTR trafficking. UC analysis of jejunal tissue revealed a significant increase in CFTR-ion transport in SGK1fl/wt mice following 1 h of DEX-treatment. PBS- and DEX-treated SGK1fl/fl mice exhibited reduced CFTR function. Conclusion: SGK1 pathway regulates CFTR in the intestine, influencing its expression, trafficking, and function. DEX-induced SGK1 activation in SGK1fl/wt mice

enhanced CFTR protein levels and ion transport, particularly at 1 h. The unexpected CFTR increase in SGK1fl/fl mice suggests compensatory roles for SGK2 and SGK3, though CFTR function remained impaired. These findings highlight SGK1 signaling as a key regulator of CFTR in the intestine.

Tetrahydrocannabinol Modulates Inflammatory Gene and miRNA Expression in HIV/SIV

Amir Valizadeh

With Rebecca T. Veenhuis, Brooklyn A. Bradley, Ke Xu

Tetrahydrocannabinol (THC), the primary psychoactive compound in cannabis, has shown promise as an immunomodulatory agent in the context of simian immunodeficiency virus (SIV) infection. In macaque models, chronic THC administration significantly altered host gene and microRNA (miRNA) expression profiles across multiple tissues. Transcriptomic analyses revealed downregulation of pro-inflammatory genes such as TNF, DEFA4, and MMP8, alongside upregulation of anti-inflammatory and tissue-repair genes including TGFB2 and TIMP2. THC also modulated miRNAs implicated in immune regulation, with several differentially expressed miRNAs targeting genes involved in cytokine signaling, epithelial integrity, and immune cell trafficking. Pathway enrichment analyses highlighted biological processes related to inflammation, epithelial barrier function, and cell adhesion. These findings suggest that THC may attenuate chronic immune activation and promote mucosal healing in SIV infection through coordinated transcriptional and epigenetic mechanisms. This work supports further investigation into THC's therapeutic potential for managing inflammation-associated complications in lentiviral infections.

Acknowledgments: Funded by the National Institute on Drug Abuse [R01-DAR01DA05284 (Xu), R01-DA038632 (Xu), R01-DA61926 (Xu and Aouizerate), R01-DA61995 (Xu and Sinha), R01-DA047063 (Xu and Aouizerat), R01-DA047820 (Xu and Aouizerat)]. Additional supports include R01-DA020419 and R01-DA030053 (Molina).

Selected Posters

Comparison of Emotion Regulation in Individuals with Obsessive-Compulsive Disorder and Non-Psychiatric Controls: An Ecological Momentary Assessment Study

Nicola Hohensee

With Claudia Bischof, Fanny Dietel, Nadja Klein, Philipp Doebler, & Ulrike Buhlmann

Emotion dysregulation is a central process implicated in the genesis and maintenance of obsessive-compulsive disorder (OCD). However, past research on OCD has examined emotion regulation with a trait-level approach, thereby neglecting important situational and temporal dynamics. The present study is the first one to examine moment-to-moment emotion regulation in individuals with OCD. A 6-day ecological momentary assessment was used to assess affect, emotion regulation strategies, and perceived effectiveness of emotion regulation strategies in n = 72 individuals with OCD and n = 54 psychologically healthy controls. As expected, individuals with OCD reported more negative and less positive affect. Group differences in positive (but not negative) affect did remain significant when controlling for baseline depression. Furthermore, the OCD group reported to use a higher momentary number of avoidance-oriented regulation strategies and less perceived effectiveness of emotion regulation, even when

controlling for current symptoms and negative affect or baseline depression scores. Further, irrespective of group, more momentary negative affect amplified use of avoidance-oriented strategies and diminished perceived effectiveness of regulatory strategies. Contrary to expectations, these effects were not more pronounced in the OCD group. Possible explanations for unexpected findings and implications for future research, particularly regarding more holistic emotion regulation treatments, are discussed.

Acknowledgments: We thank Hannah Marshall for her edits on the paper, as well as Annika Schroeder, Nora Eisenmenger, Kimberly Witte, and Max Zwigart for their support in programming, data collection, data analysis, and proofreading of the manuscript at the University of Muenster.

Characterizing the replication machinery of extrachromosomal DNA replication

Xue Jin

Extrachromosomal DNA (ecDNA) amplifications play a pivotal role in tumorigenesis by driving high-level oncogene expression, promoting tumor progression, and contributing to therapeutic resistance and poor clinical outcomes. Pan-cancer whole-genome sequencing analyses have revealed that ecDNA is present in nearly all human solid tumor types. Notably, in prostate, breast, and colorectal cancers, ecDNA prevalence is elevated in both treated cancers and untreated metastases. These findings suggest that ecDNA confers a selective advantage to tumors, making it an attractive therapeutic target. Unlike chromosomal DNA, ecDNA replication follows unique temporal and spatial dynamics. It primarily replicates within the first two hours of the eight-hour DNA replication phase and undergoes relocation from the nuclear periphery to more central nuclear regions during replication. These characteristics suggest that ecDNA replication is distinct from chromosomal DNA replication, presenting a potential for targeted therapy. However, the molecular mechanisms underlying ecDNA replication remain poorly understood. This project aims to elucidate the protein complexes and origin sequences responsible for initiating ecDNA replication. Aim 1: I employed CRISPR-dCas9-based proximity labeling to identify key replication-associated proteins. Using single guide RNA, biotin-based labeling and mass spectrometry, I will label proteins in proximity to ecDNA loci during the first two hours of ecDNA replication, profile the associated protein complexes, and validate candidate proteins through functional assays. Aim 2: I will conduct computational motif analysis on cancer patient-derived ecDNA sequences to identify replication origins. By integrating structural variant mapping with motif discovery tools, I will pinpoint the sequences that initiate ecDNA replication. These potential motifs will be validated using nucleotide incorporation assays. This study will provide the unique replication mechanisms of ecDNA, uncover novel therapeutic targets, and establish a foundation for future ecDNA-directed cancer therapies aimed at inhibiting ecDNA replication to mitigate drug resistance and metastasis.

Acknowledgments: I would like to thank my supervisor, Roel Verhaak, for his unwavering support of this project. Special thanks to Dr. Hoon Kim, Dr. Eunhee Yi, Dr. Samir Amin, Dr. Kevin Johnson and Dacheng Zhao for their valuable discussions and contributions to the experimental design and performance. I am also grateful to all the members of the Verhaak Lab for their help in initiating this project. Additionally, I appreciate the support from the Department of Neurosurgery Brain Tumor Meeting team, the eDynamic team, and the Cancer Grand Challenges grant for suggestion and making this work possible.

Postnatal Enrichment Corrects Deficits in Perineuronal Net Formation and Reversal Learning in Adult Mice Exposed to Early Adversity

Tulasi Pasam

With Sumit Jamwal, Rafiad Islam, Zoe MacDowel Kasson, Sahabuddin Ahmed, Christian Bowers, Lauryn Giuliano, and Arie Kaffman

Childhood neglect is associated with cortical thinning, hyperactivity, and deficits in cognitive flexibility that persist later in life. Despite being the most prevalent form of early adversity, little is currently understood about the mechanisms responsible for these neurodevelopmental abnormalities, and no animal models have yet replicated key structural and behavioral features of childhood neglect/deprivation. To address these gaps, we have recently demonstrated that mice exposed to impoverished conditions, specifically limited bedding (LB), exhibit behavioral and structural changes that resemble those observed in adolescents who have experienced severe neglect. Here, we show that LB leads to long-term deficits in reversal learning, which can be fully mitigated by briefly exposing LB pups to enrichment (toys) in their home cage from postnatal days 14 to 25. Reversal learning failed to induce normal c-fos activation in the orbitofrontal cortex (OFC) of LB mice, a deficit that was normalized by early enrichment. Additionally, LB decreased the density of parvalbumin-positive cells surrounded by perineuronal nets (PV+PNN+) and increased the ratio of glutamatergic to inhibitory synapse densities in the OFC, deficits that were also reversed by enrichment. Degradation of PNN in the OFC of adult mice impaired reversal learning, reduced c-fos activation, and increased the ratio of glutamatergic to inhibitory synapse densities in the OFC to levels comparable to those observed in LB mice. Our findings indicate that postnatal deprivation and enrichment have diametrically opposing effects on the formation of PV+PNN+ cells in the OFC, a developmental process that programs cognitive flexibility in adulthood.

Age-, sex-, and ancestry-specific prevalence of hearing loss in UK Biobank and All of Us Research Program

Jun He

With Sharon G Curhan, MD, ScM; Gary C Curhan, MD, ScD; Renato Polimanti, PhD

Importance Hearing loss (HL) is a leading cause of global disease burden. However, there is limited information regarding differences among individuals of diverse ancestral backgrounds. Objective To assess age-, sex-, and ancestry-specific prevalence of HL in the US and UK. Design, Setting, and Participants This cross-sectional study included 827 406 participants enrolled in UK Biobank (UKB, N = 448 193) and All of Us Research Program (AoU, N = 379 213). The combined sample had a mean age of 56 years (57 in UKB; 55 in AoU) and included 58% females and 22% individuals of non-European descent. The data were analyzed between January 2 and March 2, 2025. Main Outcomes and Measures HL was defined based on electronic health records and self-reported information. HL prevalence was calculated by age group, sex, and genetically informed ancestry. Age trends and prevalence differences between sexes and ancestries were tested. Age-standardized prevalence was computed for UKB and AoU using the combined sample size of the two cohorts as the standard population. Results The overall HL prevalence was 28% in UKB (24% in females; 34% in males) and 16% in AoU (13% in females; 20% in males). Sex differences were statistically significant across all age groups in UKB, and among participants aged >55 years in AoU. Across ancestry groups, males had a higher prevalence of HL than females, except for those of African descent in the AoU sample (10% in females and 9.5% in males). The ancestry-specific prevalence was highest among those of European descent in both UKB (29%) and AoU (20%), and lowest among those of African descent (12%) in UKB and Central/South Asian descent (7.3%) in AoU. The HL polygenic risk was associated with HL in both female and male samples.

Conclusions and Relevance The age-specific prevalence of HL differs by sex and by ancestry. This study highlights that sex differences in HL prevalence should be considered in the context of ancestral background. Further studies will be needed to assess the contribution of biological and environmental factors to the age-by-sex-by-ancestry intersection in HL.

Levels of Microglial Trem2 Program Synaptic Pruning and Hippocampal Function in a Mouse Model of Early Adversity

Sahabuddin Ahmed

With Sumit Jamwal, Lauryn Giuliano, Christian Bowers, Zoe MacDowell Kaswan

Early life adversity (ELA) impairs hippocampal development and function in humans and rodents, but the mechanisms responsible for these changes are not fully understood. We have recently shown that mice exposed to ELA through limited bedding (LB), have profound deficits in microglial-mediated synaptic pruning during a critical period of hippocampal development, leading to abnormal synaptic development and hippocampal function later in life. Microglia isolated from the developing hippocampus of LB mice exhibited reduced phagocytic activity ex vivo and lower expression of the triggering receptor expressed on myeloid cells 2 (TREM2). However, it is currently unclear if reduced TREM2 expression is directly responsible for the abnormal microglial phagocytic and whether it contributes to deficits in synaptic and hippocampal function observed in adolescent LB mice. Using Trem2 knockout mice, we determined that TREM2 is responsible for about half of the synaptic engulfment deficits in LB microglia and nearly all the abnormalities in phagosome development and synaptic degradation. Transgenic mice overexpressing TREM2 normalized phagocytic activity and restored synaptic connectivity and hippocampal function in adolescent LB mice. Our findings elucidate a crucial role for microglial TREM2 in mediating abnormal synaptic pruning and hippocampal function in a mouse model of ELA and may guide the development of novel diagnostic and therapeutic interventions.

Computing Statistical Properties of Heavy Nuclei

Dallas DeMartini

With Yoram Alhassid, Cade Rodgers

Statistical properties of heavy actinide nuclei, such as uranium and plutonium, are important properties with applications to nuclear fission, astrophysical reactions, and heavy-ion collisions. Accurate theoretical calculations of these properties are necessary because experimental data on these nuclei can be sparse. However, the huge computational resources required to model such large nuclei makes it difficult to study them without making many simplifications that reduce the accuracy of the calculations. In this talk, I will give an introduction to some of the main concepts of nuclear structure and the challenges in theoretically studying these large quantum mechanical systems. I will briefly discuss our technique, the shell-model Monte Carlo, which enables accurate calculations of these large nuclei. I will also show some recent results and compare them to experimental data as well as ongoing work studying the shapes of these nuclei.

Acknowledgments:This work was supported in part by the U.S. DOE grant No. DE-SC0019521. Computational resources used for this work were provided by the National Energy Research Scientific Computing Center (NERSC), a U.S. DOE Office of Science User Facility operated under Contract No. DE-AC02-05CH11231.

The digital organization of the Golgi apparatus

Maohan Su

With Maohan Su, Abhijith Radhakrishnan, You Yan, Yuan Tian, Hong Zheng, Ons M'Saad, Morven Graham, Jeff Coleman, Jean N. D. Goder, Xinran Liu, Joerg Bewersdorf, James E. Rothman

The protein organization of the Golgi apparatus remains incompletely understood despite its well-established compartmentalized membrane architecture by electron microscopy. Using three-dimensional super-resolution 4Pi-SMS microscopy, we comprehensively localize the human golgin family of the Golgi apparatus at 10-20 nm resolution in situ. Unexpectedly, we find that the golgins are precisely organized into a tetraplex with four discrete layers, each containing a specific set of rim golgins. We observe no golgins inside the stack between its membrane-bound cisternae. Biochemically characterizing most of the golgins as isolated proteins, we find that they form anti-parallel dimers and further self-assemble into bands of multi-micron-long filaments. Based on our findings, we propose an “outside-in” physical model, the Golgin Organizer Hypothesis, which explains the Golgi stack of cisternae and its overall ribbon morphology directly from their interactions to outer surfaces of the Golgi apparatus.

Acknowledgments:We thank Yale School of Medicine CCMI for confocal and electron microscopy, Frederic Pincet, Vivek Malhotra, Ishier Raote, Iván López Montero, Min Wu, Anup Parchure for discussions.

Insights from genome-wide high-throughput CRISPR screening study in Dyt1 Dystonia

Chandrayee Mukherjee

With Dylan Poch, Chandrayee Mukherjee, Sunanda Mallik, Vanessa Todorrow, Els Kupier, Nalini Dhingra, SheilaUmlauf, YuliaSurovtseva, Christian Schlieker

Aberrant regulation of biomolecular condensates has been linked to several incurable neurological disorders, including Amyotrophic Lateral Sclerosis (ALS), Frontotemporal Dementia (FTD), and DYT1 dystonia. Despite this, their precise role in disease etiology remains unclear. In this study, we identify MLF2-GFP as a generalizable biomarker for phase transitions, including stress granules and nuclear envelope (NE) condensates associated with dystonia. Using MLF2-GFP, we developed a high-content screening platform and computational pipeline to systematically explore regulators of NE condensates across both chemical and genetic landscapes. Through this approach, we identified RNF26 and ZNF335 as key modulators that prevent the accumulation of K48-linked polyubiquitinated proteins within NE condensates, mirroring those seen in DYT1 models. Additionally, we discovered four FDA-approved compounds that modulate condensate dynamics by promoting the clearance of ubiquitinated cargo. Our integrated chemical-genetic screen highlights zinc homeostasis—as well as potential roles for autophagy and oxidative stress—as critical factors in regulating NE phase transitions and proteostasis, pointing to new therapeutic avenues for neurological disease.

Dengue-2 mRNA-LNP vaccines protect against viral challenge in mice

Fahima Akther

With Emma Buck, Norbert Pardi, David R. Martinez

Dengue virus (DENV) remains a major global health concern, with no fully effective vaccine available against the four DENV serotypes: 1, 2, 3, and 4. The development of an effective dengue vaccine is hindered by the necessity to induce robust and balanced immunity against all four antigenically distinct DENV serotypes, as partial immunity can lead to antibody-dependent enhancement (ADE), increasing the risk of severe disease upon subsequent infections. This immunological challenge complicates both vaccine design and efficacy across diverse populations. In this study, we developed and evaluated two nucleotide-modified mRNA vaccines: prM-E-mRNA and NS1-mRNA, targeting DENV serotype 2. The prME-mRNA vaccine exhibited strong immunogenicity against whole DENV-2 virions and DENV-2 envelope protein. Moreover, both prM-E-mRNA and NS1-mRNA, administered alone or in combination, induced robust immune responses with high titers of neutralizing antibodies. Importantly, passively vaccinated immunocompetent Ifnar(-/-) mice with prM-E-mRNA and NS1-mRNA were completely protected against lethal DENV-2 infection with 100% survival. However, mice passively vaccinated with sera from the sham-control (Luc-mRNA) showed only ~15% survival. Additionally, we investigated the impact of the vaccination routes in the induction of skin tissue-resident T (Trm) cells as a frontline defender to control viral spread at the site of viral entry. We observed that intradermal (ID) vaccination induced substantially greater skin Trm cell formation compared to intramuscular (IM) delivery, with an approximately 4-fold increase following ID prime-boost immunization. These results support the potential of nucleotide-modified mRNA vaccines to induce both humoral and tissue-resident cellular immunity against DENV and warrant further investigation into long-term B and T cell responses.

Acknowledgments:-Hanna H. Gray Fellowship from the Howard Hughes Medical Institute to D. R. M - Yale Flow Cytometry Core Facility

Soil, Scat, and Sequencing: Scooping Up Hidden Mammal Ecology with eDNA

Jane Hallam

With Nyeema C Harris

Environmental DNA (eDNA) is redefining how we explore biodiversity — no binoculars required. By sampling water, soil, air, and scat, we can uncover the hidden lives of animals, parasites, and entire ecosystems. In this talk, I'll share three snapshots from my time at Yale: monitoring urban mammal diversity through soil eDNA, uncovering parasites from lion scat, and investigating the diet and gut nemabiome of North American carnivores. From city parks to African savannas, eDNA has proven a surprisingly powerful tool for revealing ecological stories we might otherwise miss. You'll leave with a new appreciation for just how much information can be found in a handful of dirt — or something even less glamorous.

Acknowledgments:Many thanks to Professor Nyeema C Harris, all past and present lab members, and our site partners across Michigan, Niger, Burkina Faso, and Senegal. I'm also deeply grateful for the molecular support provided by Dr. Gisella Caccone at the YIBS Center for Genetic Analyses, and the team at the Yale Center for Genome Analysis (YCGA).

A CRISPR-based functional genomics platform interrogates anti-viral innate immunity in horseshoe bats

Zhe Zhao

With Bridget L. Menasche, Laura M. Drepanos, Renata B. Filler, Mia M. Alfajaro, Emma L. Keeler, Mario A. Peña-Hernández, Alicen Spaulding, Leonid Serebryannyy, Daniel C. Douek, John G. Doench, Craig B. Wilen

Bats are key zoonotic reservoirs, uncovering the mechanisms of viral infection in bats is critical to preventing spillover. While comparative analyses of bat genomes highlight distinctive features of their immune systems, advanced functional genomic tools are needed to comprehensively study how bats manage to coexist with viruses. We developed a genome-wide CRISPR sgRNA knockout library against horseshoe bats (Rhinolophus spp.). We challenged library cells with various viruses, and performed deep-sequencing to quantify sgRNA representation by comparing sgRNA abundance in survival samples against the mock controls. We successfully identified known virus receptors: EFNB2 for Nipah virus and NPC1 for Ebola and Marburg virus. This confirms the activity and efficiency of our sgRNA library. Applying this platform to the picornavirus Encephalomyocarditis virus (EMCV), revealed 29 host factors critical for EMCV-induced cell death, including double-stranded RNA sensing proteins (TLR3, TICAM1, UNC93B1) and apoptosis regulators (FADD, CASP8). Analysis of rabies virus (RABV) host factors in Rhinolophus cells highlighted critical mediators within the interferon signaling pathway (IRF9, IFNB1, STAT2) as essential for RABV-induced cell death. Our current systematic gene knockout studies aim to map the genetic determinants of viral susceptibility and cell death in bat cells. This work provides a valuable toolkit for studying bat immunity and their mechanisms for combating viral infections.

Acknowledgments:Funded by NCI Prime Contract No. 75N91019D00024, Task Order No. 75N91023F00016.

Investigating the function of RME8 in Parkinson's Disease

Na Wang

Parkinson's disease (PD) is the second most common neurodegenerative disorder, while the early pathomechanisms are still elusive. DNAJC13, which encodes Receptor-Mediated Endocytosis 8 (RME8) is a synaptically enriched co-chaperone. In human cell lines, it has been shown that knockdown of RME8 results in accumulation of α-synuclein, a key feature of PD. Several mutations in DNAJC13 have been identified in PD patients, thus spurring the need to explore the causal roles of RME8 in PD in vivo. In this study, we show that RME8 conditional KO (cKO) mice develop the motor behavioral and synaptic deficits which are the PD characteristics.

Electrophysiological assessment of MDMA-induced changes in social cognition and neuroplasticity in borderline personality disorder: a pilot project proposal

Alexandra Alario

With Jones KG., Fineberg SK.

Borderline personality disorder (BPD) is a stress and trauma related psychiatric disorder affecting around 2.7% of US adults (Eaton and Greene 2018). BPD is characterized by unstable interpersonal relationships and moods, as well as chronic feelings of emptiness and identity disturbances, and has etiological and symptomatic overlap with posttraumatic stress disorder (PTSD). While psychotherapies are effective at treating BPD, patients in symptomatic remission still report impaired social functioning (Zeitler, Bohus et al. 2020), signaling a need for treatments targeting social cognition. 3,4-methylenedioxymethamphetamine (MDMA) is an empathogen-entactogenic drug that induces feelings of

empathy and closeness thought to act through neurotransmitter systems like serotonin, dopamine, norepinephrine, and oxytocin. In healthy adults, MDMA reduced the recognition of negative emotions (Hysek, Schmid et al. 2014). In people with PTSD MDMA assisted psychotherapy was more effective than psychotherapy alone at improving interpersonal dynamics, affective instability, and abandonment concerns in a sample with PTSD (van der Kolk, Wang et al. 2024). These pro-social impacts may result from MDMA's neuroplastic effects (Ly, Greb et al. 2018). Due to the similar etiology and symptom overlap between PTSD and BPD, we hypothesize that MDMA may also improve interpersonal symptoms of BPD through this mechanism. The present study will be the first to assess the effects of a single dose of MDMA on electroencephalographic (EEG) measures of social cognition and neuroplasticity in participants with BPD. We will measure visual evoked potentials (VEPs) to probe for changes in neuroplasticity (Sumner, Spriggs et al. 2020) from before to after MDMA administration in adults with BPD. We hypothesize that MDMA will increase VEP amplitudes, indicating an increase in neuroplasticity. We will also measure neural responses during a facial emotion recognition task to probe for MDMA-induced changes in social perception and cognition. We hypothesize that MDMA will induce differential effects on the face-sensitive EEG component during the face emotion recognition task and reduce negative bias in behavioral outcomes. This open label pilot study will lay the groundwork for future randomized clinical trials by characterizing MDMA's impact on social cognition in BPD.

Identifying Suicidal Young Adults using Nonverbal Behaviors: A Machine Learning Approach

Da-eun Leee

With Ilana Gratch, Jeff Cohn, Christine B. Cha

Suicide is a significant global health concern, and timely identification of individuals at risk is vital. Traditional suicide risk assessments primarily rely on self-reports, which often result in underreporting due to stigma or lack of self-awareness. While researchers have explored behavioral markers, nonverbal behaviors have been overlooked, despite their rich affective and interpersonal information. This may be because analyzing nonverbal behaviors is labor-intensive and subjective. Advances in machine learning (ML) offer promising opportunities to analyze these cues objectively and efficiently. This study aims to distinguish between suicidal and non-suicidal young adults by analyzing their nonverbal behaviors using ML. Video data were collected from 66 young adults during a semi-structured interview about suicidal thoughts and behaviors. Participants were classified into suicidal and non-suicidal groups based on the Columbia-Suicide Severity Rating Scale. Logistic Regression (LR) and Support Vector Machine (SVM) models were trained using nonverbal features, i.e., facial actions and head movements, and self-reported depression scores. LR outperformed SVM, likely due to the simplicity of the LR for optimization. Depression scores alone achieved sufficient performance, but adding nonverbal cues improved performance across all metrics. Nonverbal behaviors may add value to the identification of suicidal youth, and may help inform early-stage suicide prevention strategies.

Acknowledgments:National Institute of Mental Health (F31MH127887, PI Gratch; Co-Sponsors Cohn & Cha)

Engineering cRIPTACs for Tumor-Selective Activity and Resistance Bypass in Cancer

Skye Montoya

With Davis Chase, Maxime Mivelaz, Karolina Vankova, Ryan Tsai, Vicky Cantu, Craig Crews

Targeted protein degradation (TPD) has emerged as a powerful therapeutic strategy for eliminating oncogenic proteins, offering advantages over traditional small-molecule inhibitors, which often require continuous target occupancy and are prone to acquired resistance. However, many degraders still lack tumor specificity and risk harming normal tissues. This challenge often stems from targeting ubiquitously expressed proteins, leading to systemic toxicity. One such target is GSPT1, an essential translation termination factor whose degradation via immunomodulatory drugs (IMiDs) induces apoptosis in cancer cells but also raises concerns about on-target effects in healthy tissues. To address these limitations, we developed covalent-Regulated Induced Proximity Targeting Chimeras (cRIPTACs), a new class of bifunctional molecules engineered to enhance tumor selectivity and overcome resistance driven by bypass signaling mechanisms. cRIPTACs function via a two-step mechanism: they first covalently bind a tumor-enriched oncoprotein, such as BTK, EGFR, or KRAS, which then triggers the release of a GSPT1-targeting IMiD degrader, confining degradation to cancer cells and reducing systemic exposure. We hypothesize that cRIPTACs can overcome key limitations of both inhibitors and traditional degraders by selectively eliminating oncoprotein-expressing tumor cells while sparing normal tissue. To test this, I collaborated with a chemist in our lab to perform structure–activity relationship (SAR) studies aimed at optimizing linker architecture, covalent warheads, and payload release. Each cRIPTAC has been functionally characterized through HiBiT-based GSPT1 degradation assays, cell viability profiling to determine therapeutic index, and evaluation in established models of EGFR inhibitor resistance. Together, these findings support cRIPTACs as a promising strategy for achieving tumor-selective degradation and overcoming therapeutic resistance in cancer, with broad potential for application across refractory disease settings.

Increasing happiness through conversations with artificial intelligence

Joseph Heffner

With Chongyu Qin; Martin Chadwick; Chris Knutsen; Christopher Summerfield; Zeb Kurth-Nelson; Robb B. Rutledge

Chatbots powered by artificial intelligence (AI) have rapidly become a significant part of everyday life, with over a quarter of American adults using them multiple times per week. While these tools offer potential benefits and risks, a fundamental question remains largely unexplored: How do conversations with AI influence subjective well-being? To investigate this, we conducted a study where participants either engaged in conversations with an AI chatbot (N = 334) or wrote journal entries (N = 193) on the same randomly assigned topics and reported their momentary happiness afterward. We found that happiness after AI chatbot conversations was higher than after journaling, particularly when discussing negative topics such as depression or guilt. Leveraging large language models for sentiment analysis, we found that the AI chatbot mirrored participants' sentiment while maintaining a consistent positivity bias. When discussing negative topics, participants gradually aligned their sentiment with the AI's positivity, leading to an overall increase in happiness. We hypothesized that the history of participants' sentiment prediction errors—the difference between expected and actual emotional tone when responding to the AI chatbot—might explain this happiness effect. Using computational modeling, we find the history of these sentiment prediction errors over the course of a conversation predicts greater post-conversation happiness, demonstrating a central role of emotional expectations during dialogue. Our findings underscore the effect that AI interactions can have on human well-being.

Acknowledgments:We thank Antonia Paterson, Jonas Paul Schoene, Thomas Costello, Laura Globig, the Google DeepMind NeuroLab, and the Rutledge Lab for helpful comments.

Human ELF4 deficiency illuminates its role in inflammasome biology

Dinesh Babu Uthaya Kumar

With Angela Morka, Sindhura Siddapureddy, Sam J. Olyha, and Carrie L. Lucas

We recently discovered a novel human inborn error of immunity (IEI) caused by loss-of-function variants in the X-linked ELF4 transcription factor. Pediatric male patients with Deficiency in ELF4, X-linked (DEX) suffer from recurrent fevers, oral ulcers, and mucosal-inflammation. Elevated CXCL1, IL-6, IL-18, and IL-12/IL-23, as well as clinical responsiveness to TNFalpha, IL-1, or IL-12p40 blockade, have been observed in DEX patients. To better understand the function of ELF4, we have generated mouse models of DEX. ELF4-deficient mouse macrophages exhibit a hyperinflammatory phenotype—yet the molecular drivers remain unclear. To address this question, we performed RNA-, ATAC-, and Cut-and-Run sequencing analysis of LPS-stimulated ELF4-deficient macrophages and wild-type (WT) macrophages. Here, we observed robust changes in the transcriptome, chromatin-accessibility, and epigenetic state of macrophages—including but not limited to effects on known pro-inflammatory genes. Specifically, in ELF4-deficient macrophages compared to WT-macrophages we find: (a) reduced chromatin-accessibility, (b) diminished H3K4me3 and K3K27ac occupancy, (c) reciprocal regulation between Ifnb1 (attenuation) and IL-1β/IL-18 (activation), and (d) a substantial enrichment in the Nod-like receptor (NLR) pathway. In vitro, both ELF4-deficient macrophages and neutrophils exhibited elevated inflammasome cytokine maturation in response to ATP/Nigericin but not flagellin, poly[dA-dT], or Val-boroPro at the concentrations tested. Notably, exogenous IFN-beta1 addition to ELF4-deficient cells attenuated inflammasome activity to WT levels. Thus, we have discovered a key role for the ELF4 transcription factor in regulating the magnitude of inflammasome activation in myeloid cells, providing insights into basic biology and offering potential therapeutic targets for inflammatory diseases.

Blood-based protein biomarkers of sickle cell disease pain: A systematic review and meta-analysis

Mona Mirbeyk

With Mona Mirbeyk, MD, Shubham Misra, PhD, Geethika Koneru, MBBS, MD, MPH, Melissa C. Funaro, MS, MLS, Srikant Rangaraju, MBBS, MS, and Nitya Bakshi MBBS, MS

Pain is a major complication of Sickle Cell Disease (SCD), a rare inherited blood disorder where sickle-shaped blood cells cause vasoocclusion in blood vessels with associated ischemia and infarction, resulting in an acute vasooclusive pain episode (VOE). Most adults with SCD also develop chronic pain (CP). We conducted a systematic review and meta-analysis (PROSPERO CRD42024535776) to evaluate blood-based protein biomarkers of SCD pain in three clinical contexts: with VOE (Objective 1), by frequency of VOE (Objective 2), and with CP (Objective 3). We searched five electronic databases through 26th November 2024. The search yielded 151 eligible observational studies on 159 biomarkers, including 10,208 persons with SCD. Most biomarkers were evaluated during acute pain and were biomarkers of pain biology, inflammation, immune activation, coagulation, and hemolysis or tissue damage. We calculated a pooled standardized mean difference (SMD) and 95% CI for each protein biomarker. A meta-analysis was conducted for biomarkers reported in 2 or more studies: 80 biomarkers for Objective 1, seven for Objective 2, and four for Objective 3 respectively. We found 28 biomarkers with higher and 2 with lower levels in VOE compared to steady state. No biomarker was associated with frequency of

VOE, or with chronic SCD pain. Most (90.7%) included studies had moderate or high risk of bias using the Joanna Briggs tool modified for this study. No study used broad proteomic platforms. We also provide recommendations for best practices for reporting on biomarkers in SCD pain, and suggestions for future inquiry.

Disproportionate use of polysubstance combinations varies by sexual identity among US adults

Luis Mestre

With Juhan Lee, Maria A. Parker, Marney A. White, & Krysten W. Bold

Polysubstance use is a major public health issue affecting lesbian, gay, and bisexual (LGB) adults, especially LGB female adults. This study aims to identify the commonly used polysubstance combinations by LGB adults in the past 30 days and to determine whether these combinations differ by sexual identity and sex. Our analytic sample consisted of NSDUH 2021 and 2022 (n=66,634 adults; 8.59% LGB adults). We used survey-weighted multinomial logistic regression models to assess the polysubstance combinations by sex. The most used substances were binge alcohol drinking, cannabis, cigarettes, and nicotine vape. Bisexual female adults used most of the assessed polysubstance combinations that included binge alcohol drinking, cannabis, or both, often involving three or four substances. Sex differences among the polysubstance combinations vary among heterosexual and bisexual adults but not among gay/lesbian adults. Public health strategies must consider the specific sexual identity, sex, and the types of substance combinations involved.

Decoding Rare CNVs and Their Functional Insights in Major depressive disorder from Latin American Cohorts

Diana Núñez

With Diana L Núñez-Ríos, Sheila T Nagamatsu, José Jaime Martínez-Magaña, Humberto Nicolini, Alma Delia, Maria C Lattig, Yvonne Marquez, Eugenio Ferro, Karen G Martinez, Paola Guisti, LAGC-MDD group, PGC-CNV group ,Thomas Fernandez & Janitza L Montalvo-Ortiz

Copy-number variations (CNVs) are genetic rearrangements that result in the loss or gain of DNA sequences larger than 50 nucleotides. Like single nucleotide variants (SNVs), CNVs contribute to genetic diversity and can influence disease risk. MDD, a mood disorder affecting 15% of the global population and 12.58% of Latin American population, has an estimated heritability of 37%. While genome-wide association studies (GWAS) have identified SNVs associated with MDD, most CNV studies focus on burden analysis without exploring individual variants or their functional impacts. Moreover, the predominance of European ancestry in genetic studies limits insights into diverse populations, including admixed Latin Americans. To address these gaps, we analyzed rare CNVs in MDD cases and controls from Latin America, focusing on dosage-sensitive genes with potential functional relevance. Methods: We studied 947 MDD cases and 310 controls from cohorts in Colombia, Mexico, Puerto Rico, including 525 males and 732 females. 32 samples from the UTHealth cohort were also included in the analysis. CNVs were detected using PennCNV and genoCN, retaining only CNVs with ≥70% overlap between methods. Using PLINK, we filtered CNVs with a frequency below 1% and analyzed burden association across cases and controls. Gene annotations were performed using the UCSC genome database (hg38). CNVs mapping to dosage-sensitive genes were filtered using the gnomAD database, and CNVs mapping MDD-associated genes were filtered using GWAS catalog database. Functional relevance was assessed based on CNV characteristic and gene mapped regions. Ancestry inference was performed separately for

each cohort using KING and the 1000 Genomes Project data as a reference panel. Results: Complex admixture patterns within and between Latin American (LA) populations were observed in the ancestry PCA plots where samples from Mexico and Colombia showed distinct distributions compared to those from Puerto Rico. When comparing CNV distribution between cases and controls, we observed a larger number of CNVs per individual in cases, with case-to-control ratios of 4.68:1 for deletions and 1.6:1 for duplications. No differences in number of CNVs were found between males and females. As previous studies have reported, the filtered CNVs in LA cohorts were significantly enriched for NDD-associated CNVs ($p = 0.004$). We also found a significant enrichment for genes implicated in MDD ($p = 5.8 \times 10^{-8}$) and for dosage-sensitive genes with pLI values greater than 0.8 ($p = 5.3 \times 10^{-16}$). To identify rare CNVs with potential clinical relevance in MDD, we first selected CNVs with a frequency below 10% that overlapped either NDD-associated regions, MDD-associated gene and dosage sensitive genes. After this filtering, we identified CNVs mapping to four neurodevelopmental disorder (NDD)-associated loci—1p36, 22q11, 11p15.5, and 22q13.33—that were overrepresented in cases compared to controls in at least two of the analyzed cohorts. Additionally, we identified CNVs intersecting MDD-associated and dosage-sensitive genes in the regions 1p36.22, 12q14, 16q24, 17p11, 17q25, and 19q13. Notably, some CNVs in these regions shared identical breakpoints across multiple samples; however, comparison with existing databases revealed that these breakpoints did not coincide with known segmental duplications. Further investigation into segmental duplications within admixed populations will be necessary to determine whether these CNVs represent recurrent events in our study population. We also confirmed that the selected CNVs overlap with coding regions and did not exhibit a 100% overlap with CNVs reported in the curated Gold Standard Database of Genomic Variants. Based on our observations and following ACMG (American College of Medical Genetics and Genomics) guidelines, these variants can be classified as either variants of uncertain significance (VUS) or likely pathogenic (LP). Among the genes affected by these VUS/LP CNVs, we identified NF2, DEAF1, PHRF1, ELAVL1, RBFOX3, and RAI1, all of which are highly expressed in the brain and play roles in neurodevelopment or gene regulation. Conclusion: This study demonstrates the value of examining CNVs based on their inherent characteristics rather than restricting analyses to burden assessments. We prioritized rare CNVs mapping to known NDD-associated CNVs, MDD-associated genes discovered via GWAS and dosage-sensitive genes to uncover candidate genes potentially involved in MDD. Expanding sample sizes in the understudied Latin American populations, will further enhance the discovery of risk variants and the understanding of CNV population stratification.

Acknowledgments:This study was supported by the National Institute on Drug Abuse R21DA050160 and DP1DA058737 (J.L.M.O.); the U.S. Department of Veterans Affairs via the National Center for Posttraumatic Stress Disorder – Veterans Affairs Connecticut (J.L.M.O.), 1IK2CX002095-01A1 (J.L.M.O.), and the Kavli Institute for Neuroscience at Yale University Kavli Postdoctoral Award for Academic Diversity (J.J.M.M.). This publication was made possible in part by the Yale Center for Brain and Mind Health, which is sponsored by the Yale School of Medicine (D.L.N.R.).

Postnatal Enrichment Corrects Deficits in Perineuronal Net Formation and Reversal Learning in Adult Mice Exposed to Early Adversity

Tulasi Pasam

With Sumit Jamwal, Rafiad Islam, Zoe MacDowel Kasson, Sahabuddin Ahmed, Christian Bowers, Lauryn Giuliano, and Arie Kaffman

Childhood neglect is associated with cortical thinning, hyperactivity, and deficits in cognitive flexibility that persist later in life. Despite being the most prevalent form of early adversity, little is currently understood about the mechanisms responsible for these neurodevelopmental abnormalities, and no animal models have yet replicated key structural and behavioral features of childhood neglect/deprivation. To address these gaps, we have recently demonstrated that mice exposed to impoverished conditions, specifically limited bedding (LB), exhibit behavioral and structural changes that resemble those observed in adolescents who have experienced severe neglect. Here, we show that LB leads to long-term deficits in reversal learning, which can be fully mitigated by briefly exposing LB pups to enrichment (toys) in their home cage from postnatal days 14 to 25. Reversal learning failed to induce normal c-fos activation in the orbitofrontal cortex (OFC) of LB mice, a deficit that was normalized by early enrichment. Additionally, LB decreased the density of parvalbumin-positive cells surrounded by perineuronal nets (PV+PNN+) and increased the ratio of glutamatergic to inhibitory synapse densities in the OFC, deficits that were also reversed by enrichment. Degradation of PNN in the OFC of adult mice impaired reversal learning, reduced c-fos activation, and increased the ratio of glutamatergic to inhibitory synapse densities in the OFC to levels comparable to those observed in LB mice. Our findings indicate that postnatal deprivation and enrichment have diametrically opposing effects on the formation of PV+PNN+ cells in the OFC, a developmental process that programs cognitive flexibility in adulthood.

Fast, accurate 3D neuron simulations across multiple meshes

Cecilia Romaro

With Robert A. McDougal

The moment-to-moment operation of the brain involves the generation, propagation, and interaction of electrical and chemical signals in time and space. Anatomical complexity poses a special challenge for chemical signals because relevant structures in an individual cell can range from < 1 um to > thousands of um. We have developed methods that achieve accurate and efficient simulation by constructing multiscale cubic meshes tailored to a model's anatomical complexities. We present an algorithm (implemented inside the NEURON simulator; nrn.readthedocs.io) that achieves independent mesh discretization over different regions of a cell. This permits smooth diffusion of chemical signals between meshes while preserving conservation of mass and numerical accuracy. We also address subtle issues arising in the interpretation of results, such as those due to discrepancies in estimated volumes between two meshes, as well as runtime performance and numerical stability.

Acknowledgments:This research was funded by the National Institute of Mental Health, National Institutes of Health, grant number R01 MH086638. The content is solely the responsibility of the authors and does not necessarily represent the official views of the National Institutes of Health.

Analyzing Yale University Reproductive Sciences Biobank Data vs. the General Population: Identifying Gaps and Advancing Equitable Representation

Aliaksandr Kishchanka, M.D.

With Samantha Girasulo, B.S.

Biobanks support clinical research, but demographic disparities in participant enrollment can limit research generalizability. The Yale University Reproductive Sciences (YURS) Biobank collects OB/GYN specimens, yet representation gaps persist. Objective: This study compares the demographic

distribution of YURS Biobank participants with the general population of New Haven County to identify underrepresented groups. Methods: An analysis (2014–2021) used U.S. Census Bureau's American Community Survey (ACS) data to assess racial and ethnic disparities. Statistical tests, including chi-square and Fisher's exact tests, evaluated representational differences. Results: The YURS Biobank overrepresents White and Black participants, while Asian and Native Hawaiian/Other Pacific Islander populations remain underrepresented. Hispanic/Latino representation aligns with ACS estimates. Conclusions: While multilingual consent and interpreter services improve accessibility, targeted recruitment strategies are needed to enhance diversity. Future studies should benchmark against national biobanks and assess the impact of inclusion efforts to ensure equitable representation in biomedical research.

Single-nucleus sequencing reveals transcriptomic and chromatin accessibility alterations associated with chronic cannabis use in people with HIV

Mingrui Li

With Ying Hu, Eric O. Johnson, Bradley E Aouizerat, Ke Xu

Cannabis is highly prevalent among people with HIV (PWHs). To understand how cannabis use influences immune gene function in the context of HIV infection, we profiled single nucleus transcriptome and chromatin accessibility by 10x multiome for peripheral blood mononuclear cells from 23 PWHs, 11 cannabis users and 12 non-cannabis users. After quality control, a total of 91,842 nuclei were clustered into 7 major cell types (i.e. CD4+ T cells, CD8+ T cells, B cell, natural killer cells, classical monocytes, non-classic monocytes, and dendritic cells.) We identified 1,234 differentially expressed genes (DEGs) between chronic cannabis use and non-use. Approximately 50% of the DEGs were found only in one cell type. We further identified 4,462 differentially chromatin accessible regions (DARs) associated with cannabis use, around 75% of which were specific to one cell types. These DEGs were enriched in multiple significant pathways including immune response, cytokine production, apoptosis and inflammatory response. Integrating multiomic data, we found that multiple DEGs were correlated with DARs in specific cell types. For example, in CD4+ T cells, the expression of NFKBIA (FDR=1.31×10^(-61),log2FC=0.87) correlated with a DAR chr14:35415732-35417260 (FDR=0.0498, Log2FC= 0.17) located at NFKBIA's putative enhancer. NFKBIA plays a critical role in regulation of immune and inflammatory function. Together, our results from an in vivo human study demonstrate that cannabis modulates immune and inflammation function via altering epigenetically regulated cell-type-specific transcriptomes, providing new insights of immune mechanisms of chronic cannabis use in HIV infection.

Single nucleus transcriptome and chromatin analysis identifies frontal cortex differentially expressed genes for SIV infection in rhesus macaques

Xiaoke Duan

With Rebecca Veenhuis, Mingrui Li, Bradley E. Aouizerat, Mathew J. Girgenti, Ke Xu

Simian immunodeficiency virus (SIV) infected-rhesus macaque is a well-established model for understanding the complex pathology of HIV infection. We analyzed single-nucleus RNA sequencing (snRNA-seq) and single-nucleus ATAC sequencing (snATAC-seq) of 32,358 nuclei for SIV-infection (N=6) in the brain regions of frontal cortex (FC). Our preliminary analysis found 7 major cell types, including excitatory neuron (ExcN, 22.59%), inhibitory neuron (InhN, 14.65%), astrocyte (Astro,

3.75%), microglia (Micro, 9.82%), oligodendrocyte (Oligo, 43.23%), Oligodendrocyte precursor cells (OPC, 5.38%), and vascular cells (Vasc, 0.57%). We identified 108 differentially expressed genes (DEGs) in microglia between SIV infected and non-infected macaques (FDR < 0.05) [e.g., IFI44L (avg_diff = 2.78, padj = 1.99e-122), MX1 (avg_diff = 4.14, padj = 8.37e-33), CDH13 (avg_diff = -2.29, padj = 8.63e-115)]. These DEGs were enriched in significant multiple GO terms such as "response to virus" and "regulation of trans-synaptic signaling". Interestingly, snATAC-seq analysis identified differential chromatin accessibility peak near CDH13 in microglia cells between SIV-infected and non-infected macaques. The correlation of this peak and CDH13 expression is 0.11 (pvalue = 3.78e-06), suggesting that SIV infection may epigenetically regulate CDH13 expression. CDH13 plays a critical role in a negative regulator of axon growth during neural differentiation. These preliminary findings provide new insights into the region and cell-type specific transcriptomic alterations for SIV infection.

Identifying the biochemical mechanism by which opioids and other signals inhibit neural activity

Shadi Yavari

Opioids and many neurotransmitters and neuropeptides shut down neural activity by signaling through G protein-coupled receptors (GPCRs) that activate a heterotrimeric G protein, Gao. This abundant G protein is found in every neuron and constitutes ~1% of protein in the brain. All other G proteins in humans are known to signal by directly binding and regulating target proteins known generically as "effectors", but surprisingly no effector has yet been identified for Gao. The Koelle lab and others have used C. elegans genetics to identify the enzyme diacylglycerol kinase (DGK) as a potential effector of Gao. We are now testing whether purified DGK interacts with purified Gao in a manner expected for an effector:G protein interaction. Our work could provide a mechanistic understanding of how signals, including opioids, downregulate neural activity.

Spatial Proteomics of Immune Checkpoints in Discoid Lupus and Lichen Planus

Ümmügülsüm Yıldız-Altay

With Rachel Breidbart, Michal Kidacki, Anjali Jaiswal, Christina Cho, Matthew D. Vesely

Interface dermatoses a histopathological pattern observed in several autoimmune connective tissue diseases, including discoid lupus erythematosus (DLE) and lichen planus (LP). Despite distinct clinical presentations, both diseases share histologic features suggestive of common underlying pathogenic mechanisms. However, their immunoregulatory landscapes remain unclear. This study employs spatial proteomics to characterize immune inhibitory receptor expression in DLE and LP, revealing disease-specific and overlapping immune checkpoint pathways. We analyzed archival DLE and LP skin biopsies using the NanoString GeoMx Immuno-Oncology protein panel. Heatmap and UMAP clustering demonstrated distinct protein expression profiles between DLE and LP. Cross-segmentation analysis of keratinocytes (PanCK+), CD4+, and CD8+ T cells identified differential immune checkpoint and T cell activation expression. In DLE, immune modulation was compartmentalized, with keratinocytes expressing PD-L2, CD44, and CD127 compared to CD4+ and CD8 T cells. Additionally, CD4+T cells in DLE expressed greater ICOS, CTLA4, OX40L, CD40, 4-1BB, and PD-1 compared to CD8+ T cells. In contrast to DLE, CD4+ and CD8+ T cells within LP tissues expressed VISTA, PD-L1, and STING, whereas keratinocytes express OX40L, CD127, CD44 and ARG1. These findings underscore key immunoregulatory differences in interface dermatoses and suggest potential therapeutic strategies, including immune checkpoint agonists, for targeted intervention in autoimmune dermatoses.

A Simple Method for Generating Droplets on a Vibrating Liquid Bath

Johnathan Hoggarth

With D.M. Harris, J.W.M. Bush, B.K. Primkulov

The breakup of a thin liquid thread into droplets is a well-studied phenomenon influenced by factors such as surface tension and viscosity. We investigate the controlled formation of a single droplet when pulling a liquid thread from a bath. Using a simple customized pen mechanism, we demonstrate a reliable method for generating single droplets of a desired radius from a bath of silicone oil. By utilizing a high-speed camera and systematically varying the pull speed and pen tip radius, we characterize the dimensions of the liquid ligament and access a wide range of droplet sizes. This method provides a straightforward approach for producing droplets on a vibrating bath, offering a simple technique for future experimental investigations.

Structural Basis for Viral Recruitment of Hypophosphorylated RNA Polymerase II for Late Gene Transcription in the Beta/Gammaherpesviruses

Pankaj Madheshiya

With Xinyu Chen, Shannon Henry, Shaogeng Tang, Allison Didychuk

Herpesviruses do not encode their own RNA polymerase and must hijack cellular RNA Polymerase II (Pol II) for expression of their protein-coding genes. Initiation of transcription is tightly controlled, starting with formation of a pre-initiation complex (PIC) wherein Pol II is recruited to the promoter. PICs on early viral promoters are thought to resemble those on host promoters. In contrast, in the beta/gammaherpesviruses, late promoters assemble a viral PIC (vPIC) dependent on six viral transcriptional activators (vTAs). One of these vTAs (ORF24 in KSHV) has a domain that mimics cellular TATA-binding protein (TBP). The TBP-like domain is distinct from its N-terminal domain (ORF24-NTD), which is necessary and sufficient for recruitment of Pol II to late promoters. ORF24-NTD directly interacts with Rpb1, the largest subunit of Pol II, and specifically binds its low complexity C-terminal domain (CTD). To understand the basis of Pol II recruitment, we determined the structure of ORF24-NTD. We find that it adopts a novel fold distinct from any known proteins outside the beta/gammaherpesviruses. We identified a conserved region of ORF24-NTD, and mutation of residues within this region disrupted the ORF24-Pol II interaction. It has previously been shown that ORF24 selectively binds to hypophosphorylated Pol II, consistent with its recruitment into a PIC. To understand the underlying mechanism allowing for selective binding to Pol II with the appropriate phosphorylation state, we extensively mutagenized the heptapeptide repeats of the Pol II CTD and measured binding of ORF24-NTD. We find that all mutations, including phosphomimetics, disrupt binding, with a particularly strong effect at positions Y1, T4, and S5 within the CTD heptapeptide repeats. We further show that ORF24 is incorporated into CTD condensates in vitro. Our results reveal how the beta/gammaherpesviruses efficiently recruit Pol II to ensure viral transcription occurs late in infection.

Acknowledgments:This research is supported by the National Institutes of Health (DP2AI171113) and the Damon Runyon Cancer Research Foundation (DRG-2349-18).

Vascular mimicry as a facilitator of melanoma brain metastasis

Olivia Provance

With Olivia K. Provance, Victor O. Oria, Thuy T. Tran, Jasmine I. Caulfield, Christopher R. Zito, Adam Aguirre-Ducler, Kurt A. Schalper, Harriet M. Kluger & Lucia B. Jilaveanu

Melanoma has the highest propensity among solid tumors to metastasize to the brain. Melanoma brain metastases (MBM) are a leading cause of death in melanoma and affect 40–60% of patients with late-stage disease. Therefore, uncovering the molecular mechanisms behind MBM is necessary to enhance therapeutic interventions. Vascular mimicry (VM) is a form of neovascularization linked to invasion, increased risk of metastasis, and poor prognosis in many tumor types, but its significance in MBM remains poorly understood. We found that VM density is elevated in MBM compared to paired extracranial specimens and is associated with tumor volume and CNS edema. In addition, our studies indicate a relevant role of YAP and TAZ, two transcriptional co-factors scarcely studied in melanoma, in tumor cell-vasculogenesis and in brain metastasis. We recently demonstrated activation of the Hippo tumor suppressor pathway and increased degradation of its downstream targets YAP and TAZ in a metastasis impaired cell line model. In the current study we establish the utility of anti-YAP/TAZ therapy in mouse models of metastatic melanoma whereby treatment effectively inhibits VM and prolongs survival of mice with MBM. The data presented herein suggest that VM may be an important and targetable mechanism in melanoma and that VM inhibition might be useful for treating MBM, an area of high unmet clinical need, thus having important implications for future treatment regimens for these patients.

Modeling Narrative Structure in Visual Stories through Hierarchical Knowledge Graphs

Yi-Chun Chen

Narrative comprehension in visual media, such as comics and educational image sequences, relies not only on visual cues but also on latent linguistic and semantic structures. This work introduces a hierarchical knowledge graph framework to represent and reason about multimodal narratives, integrating panel-level descriptions, temporal relations, and event-level abstractions. The framework links visual features with associated textual elements (e.g., captions, dialogue) to enable structured narrative analysis. Using a manually annotated subset of the Manga109 dataset, we demonstrate how this graph-based representation supports tasks such as event segmentation, character interaction modeling, and narrative flow tracking. This research builds on my doctoral work in visual storytelling and provides a foundation for ongoing exploration into how structured representations can enhance language understanding in multimodal domains. This work also informs my current research direction in structured language understanding within multimodal contexts.

Acknowledgments:This work builds on my doctoral research at NC State University and is supported by my current postdoctoral position in the Department of Emergency Medicine at Yale University.

Organizers

The 2025 Yale Postdoctoral Association Symposium was organized by

Jacob Orkwis, PhD. (Co-coordinator)

Adati Tarfa, PharmD, MS, PhD. (Co-coordinator)

Annubha Seth, PhD. (Events Sub-committee leader)

Danielle Sohai, PhD. (Judging Sub-committee leader)

Eunate Gallardo, PhD. (Scheduling Sub-committee leader)

Nicole Demarais, MD. (Communications Sub-committee co-lead)

Adina MacMahon Copas, PhD. (Communications Sub-committee co-lead)

Other Members: Dilpreet Kour PhD, Nebal Abu Hussein PhD., Tommaso Volpi PhD., Cameron Gardner PhD., Gizem Nur Sahin Kayabolen PhD., Jon Bell PhD., Jamison Leid PhD., Jiayi Xu PhD., Parvaneh Rastgou PhD., Chetna Dhembla, PhD.

About the YPA

Under the leadership of two chairs, the YPA organizes events through nine committees: Advocacy Committee, Belonging Committee, Communications Committee, Community and Networking, Mentorship Committee, Professional Development, Secretaries Committee, Symposium Committee, & Treasury Committee.

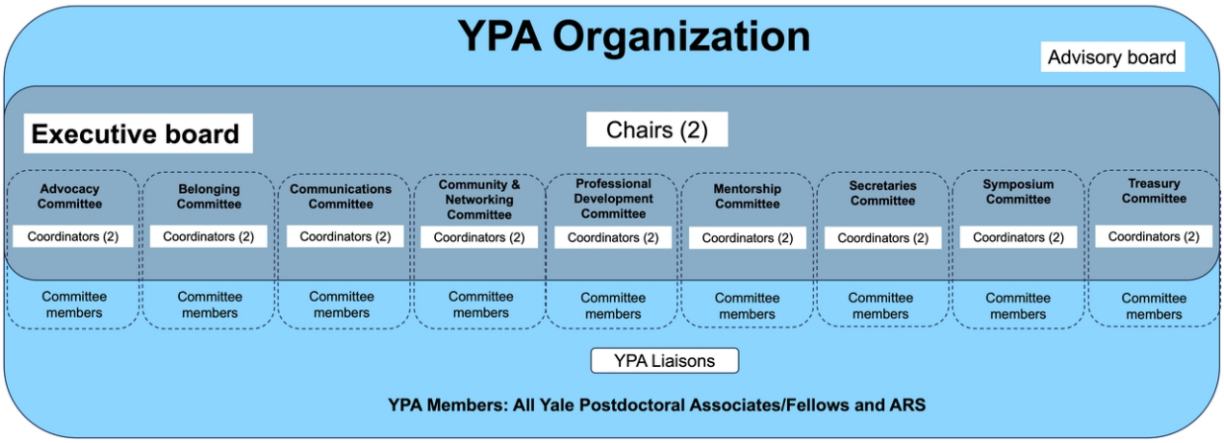

Ad-hoc subcommittees can be created by Committee Coordinators, Secretaries, and Chairs to support ongoing initiatives of existing committees. This structure helps us organize the best events for the different needs of all postdocs and their families.

Interested in learning more about the YPA? Join our Open Forums, taking place on the second Tuesday of each month. This month, we will be meeting at the Yale Science Building, Room 352, from 6 to 7pm on June 10th, 2025.

Want to get more involved? Meet other postdocs at Yale? Help plan the next Symposium? Follow us on **Yale Connect!**